Filling gaps in GW searches
new opportunities in the spectrum of GWs

Diego Blas

based on 2107.04063/2107.04601 (PRL/PRD22) and 2112.11465 (PRD22)

(w. Alex Jenkins // A. Berlin, DB, R. T. D'Agnolo, S. Ellis, R. Harnik, Y. Kahn, J. Schütte-Engel)

Universitat Autònoma de Barcelona

Barcelona Institute of Science and Technology

Ayuda Beatriz Galindo Senior
BG20/00228

GOBIERNO DE ESPAÑA
MINISTERIO DE UNIVERSIDADES

MINISTERIO DE CIENCIA E INNOVACIÓN

AGENCIA ESTATAL DE INVESTIGACIÓN

MW in visible band


MW in X rays

The Gravitational Soundscape **ca. 2040**

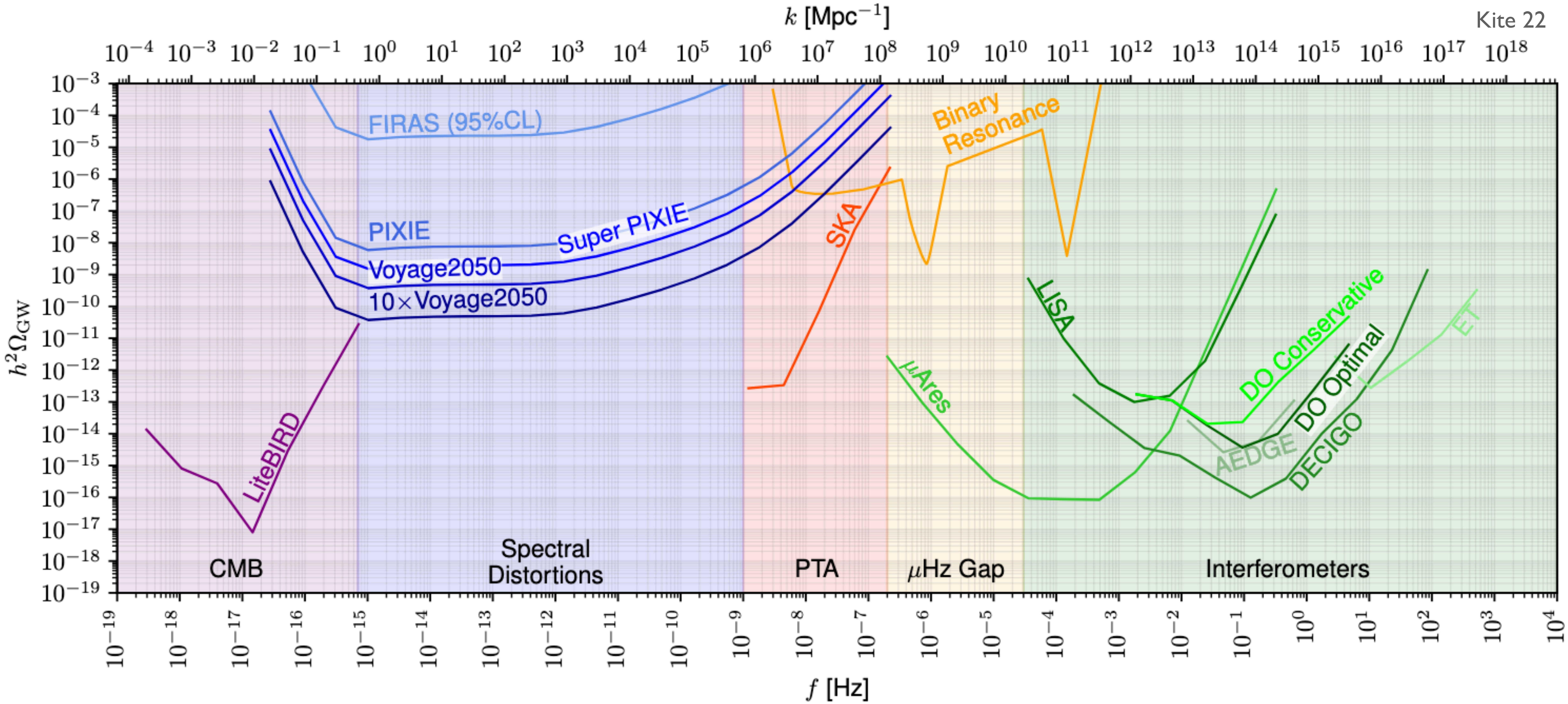

year

$$\Omega_{\rm GW}(f) = \frac{1}{\rho_{\rm crit}} \frac{{\rm d}\rho_{\rm GW}}{{\rm d}(\ln f)}$$

The Gravitational Soundscape ca. 2040

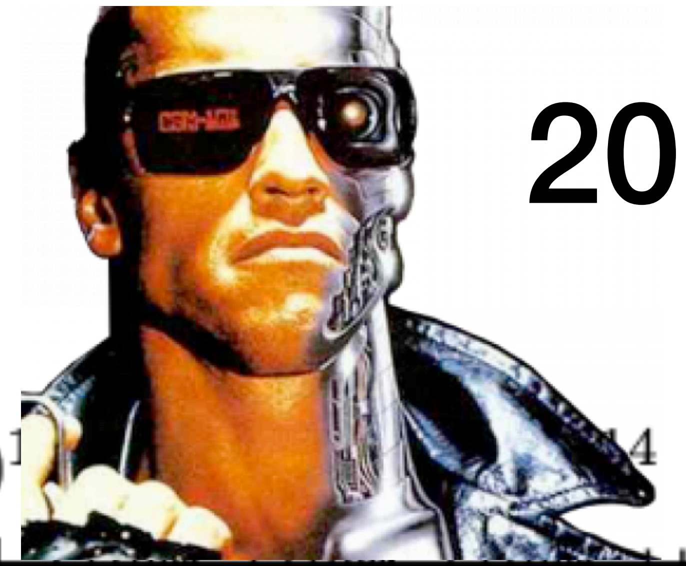

2029

Kite 22

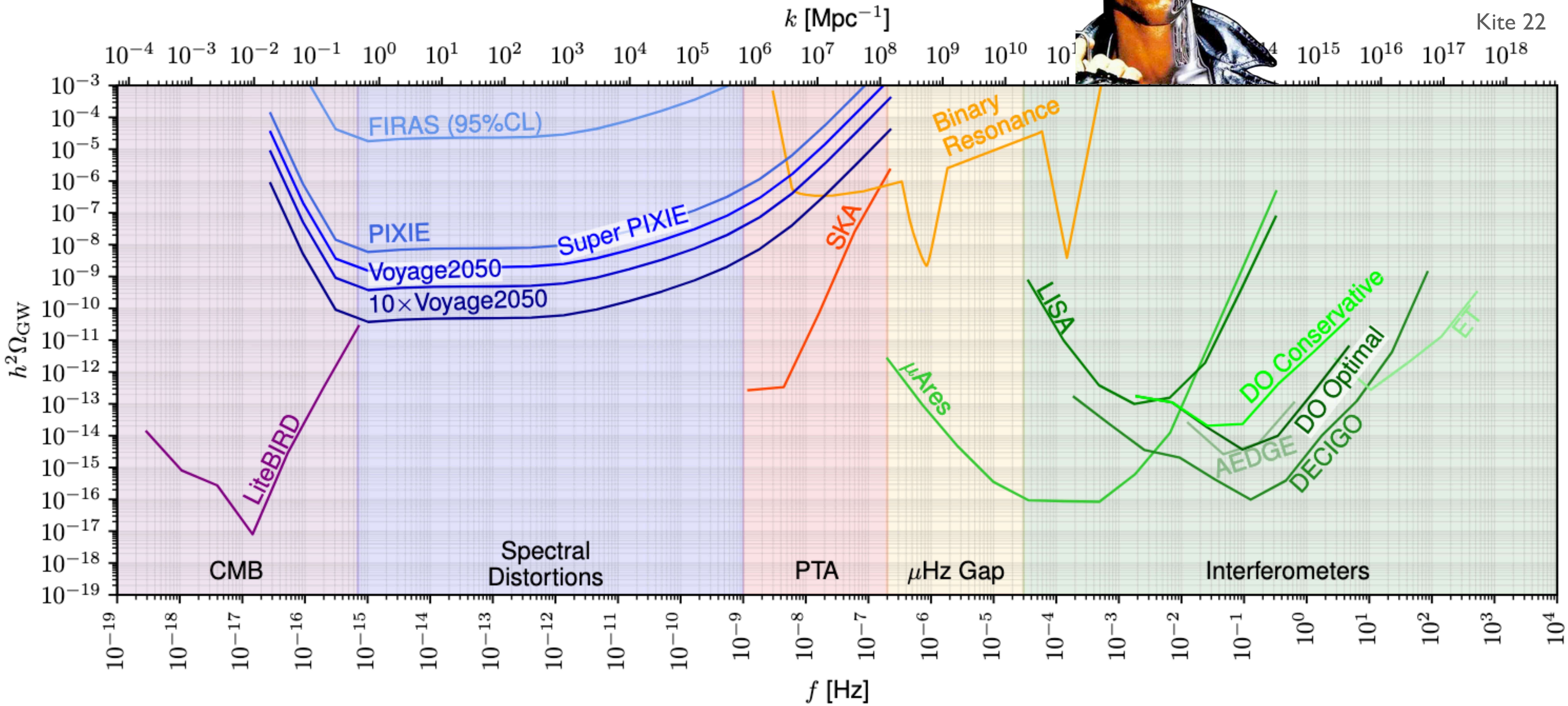

year

$$\Omega_{GW}(f) = \frac{1}{\rho_{crit}} \frac{d\rho_{GW}}{d(\ln f)}$$

The Gravitational Soundscape ca. 2040

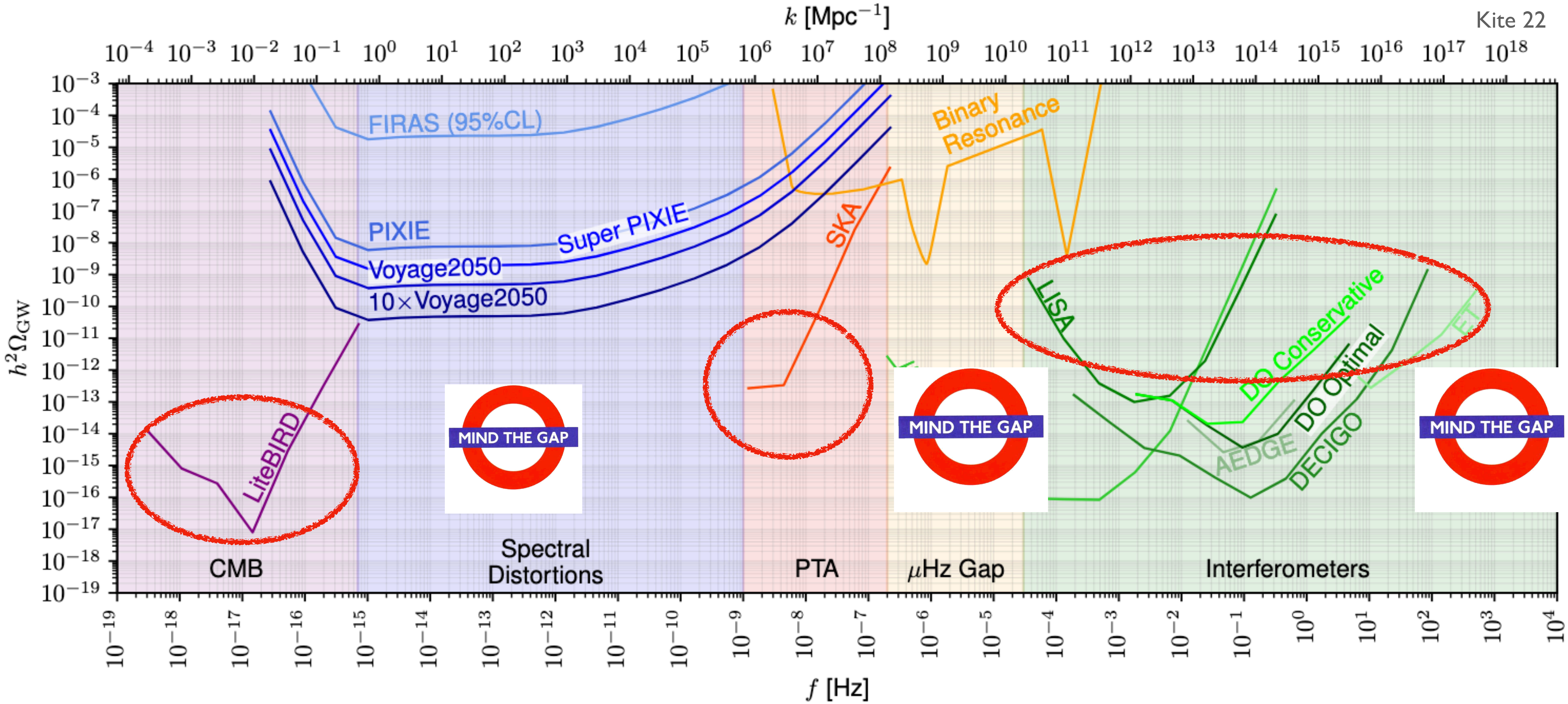

The Gravitational Soundscape ca. 2040

Kite 22

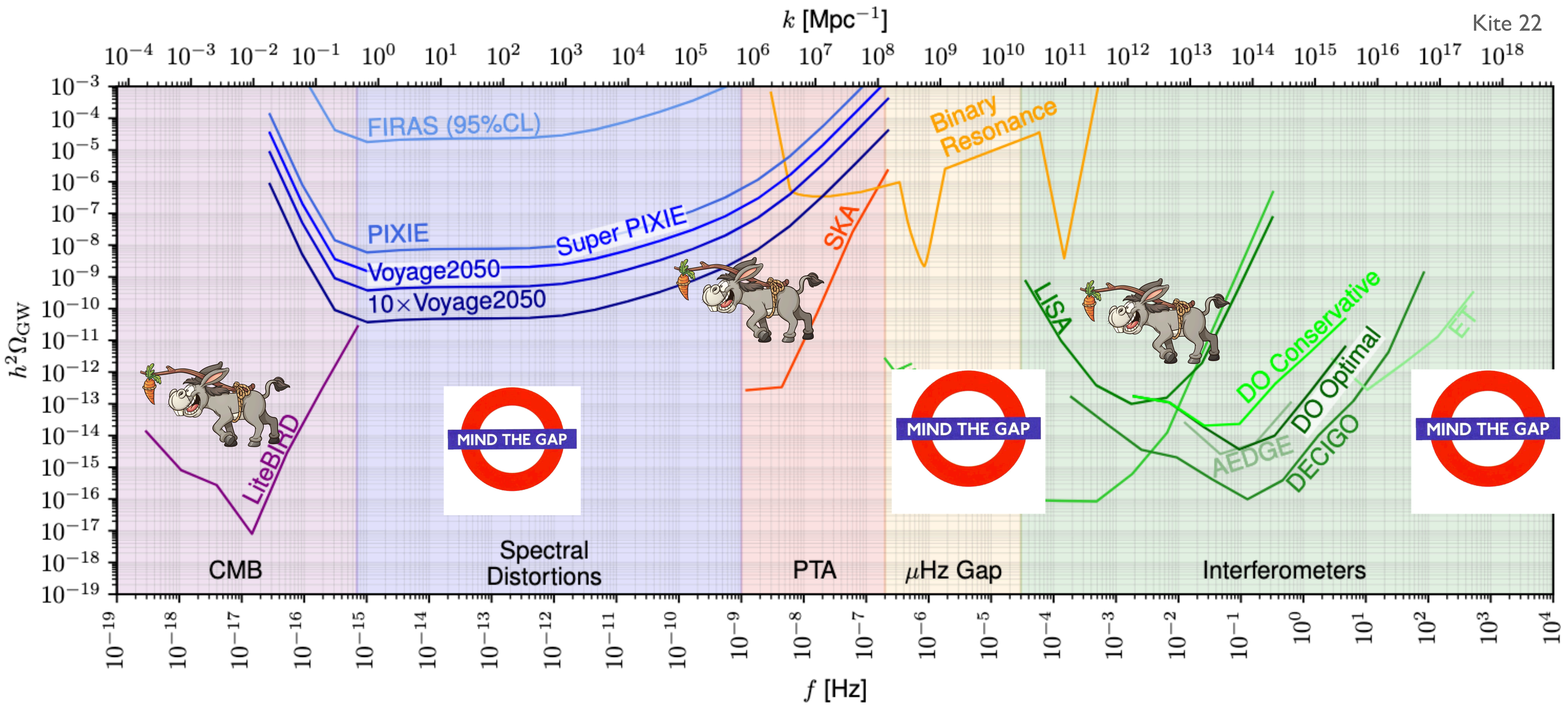

The Gravitational Soundscape ca. 2040

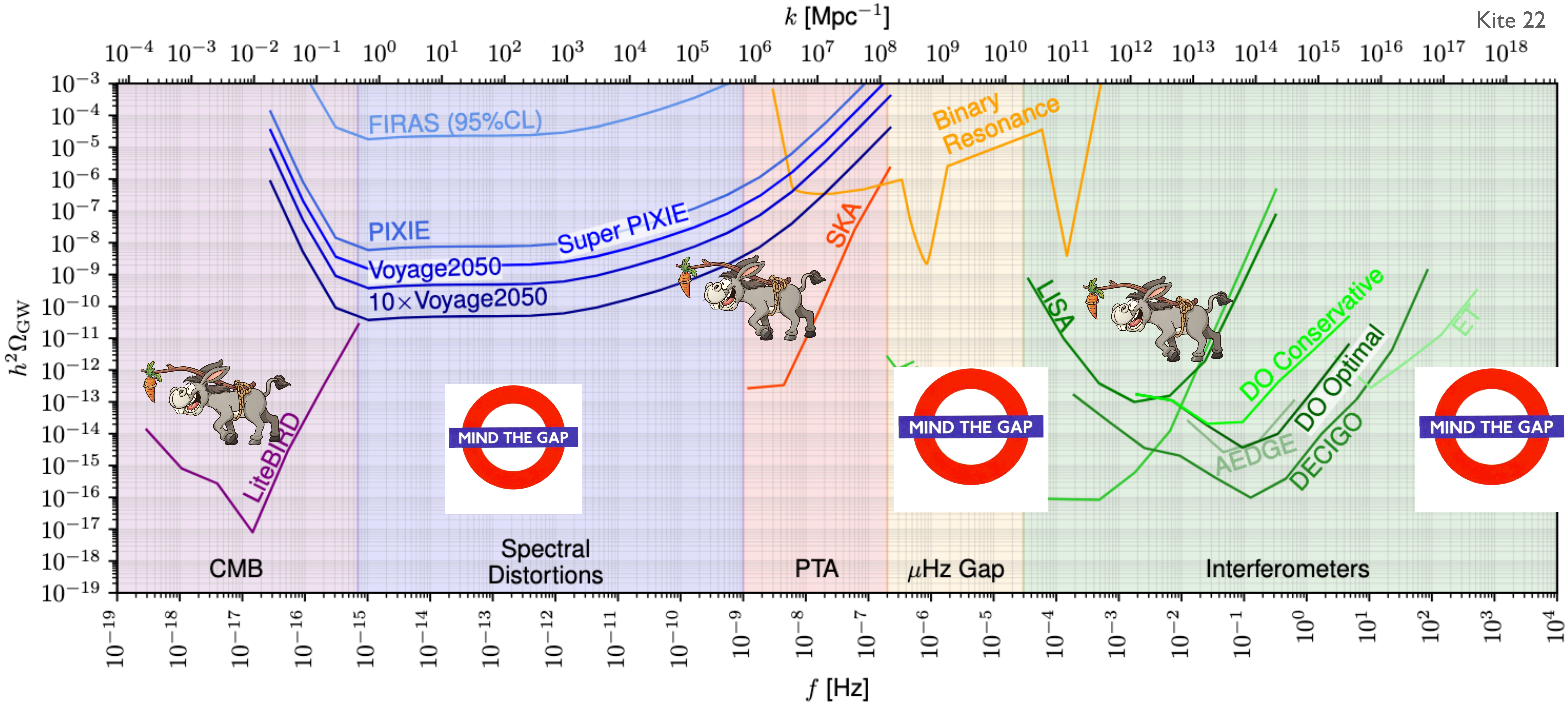

Not today….

year

part I: $\mu\mathrm{Hz}$

part II: GHz

Current SGWB constraints

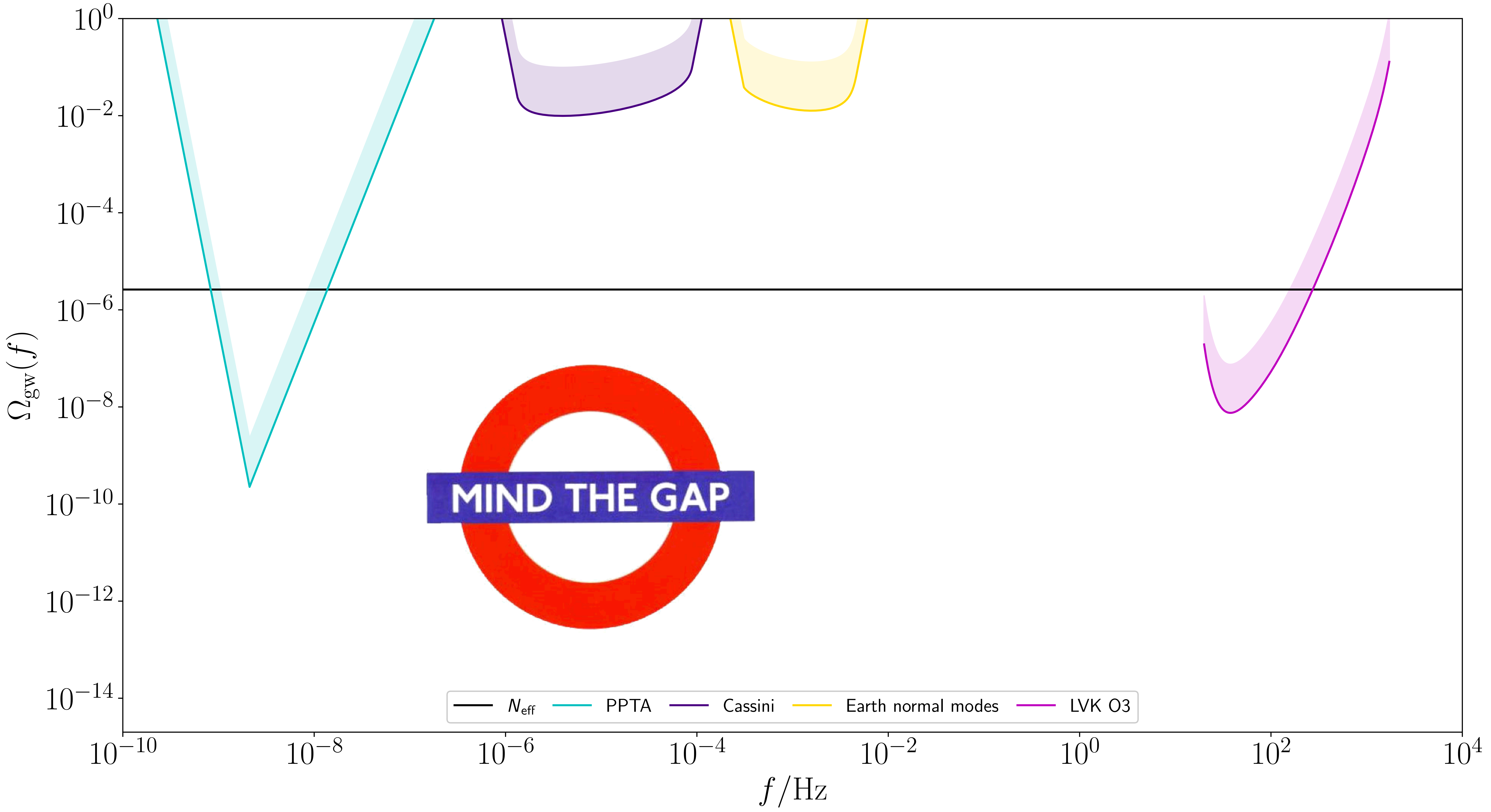

dblas@ifae.es

Binary resonance: a brief history

discussed by Misner, Thorne, and Wheeler. . .

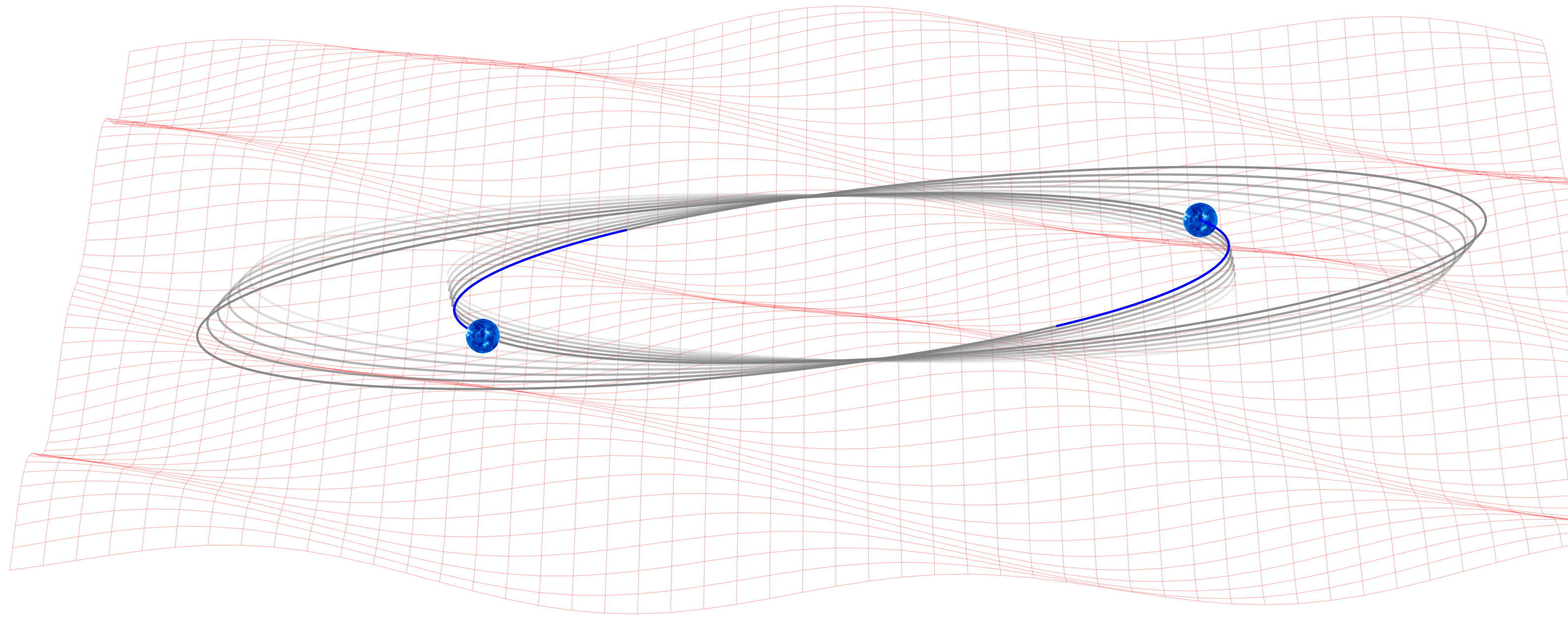

1. The Relative Motions of Two Freely Falling Bodies

As a gravitational wave passes two freely falling bodies, their proper separation oscillates (Figure 37.3). This produces corresponding oscillations in the redshift and round-trip travel times for electromagnetic signals propagating back and forth between the two bodies. Either effect, oscillating redshift or oscillating travel time, could be used in principle to detect the passage of the waves. Examples of such detectors are the Earth-Moon separation, as monitored by laser ranging [Fig. 37.2(a)]; Earth-spacecraft separations as monitored by radio ranging; and the separation between two test masses in an Earth-orbiting laboratory, as monitored by redshift measurements or by laser interferometry. Several features of such detectors are explored in exercises 37.6 and 37.7. As shown in exercise 37.7, such detectors have so low a sensitivity that they are of little experimental interest.

. . . but that was *50 years ago!*

investigated more recently by Lam Hui *et al*, PRD (2013),
similar ideas used to search for dark matter by Blas *et al*, PRL (2017)

time for a closer look?

Orbital elements

$$\ddot{\boldsymbol{r}} + \frac{GM}{r^2}\hat{\boldsymbol{r}} = \boldsymbol{\delta}\ddot{\boldsymbol{r}}. \qquad \delta\ddot{r}^i = -\delta R^i{}_{0j0}r^j$$

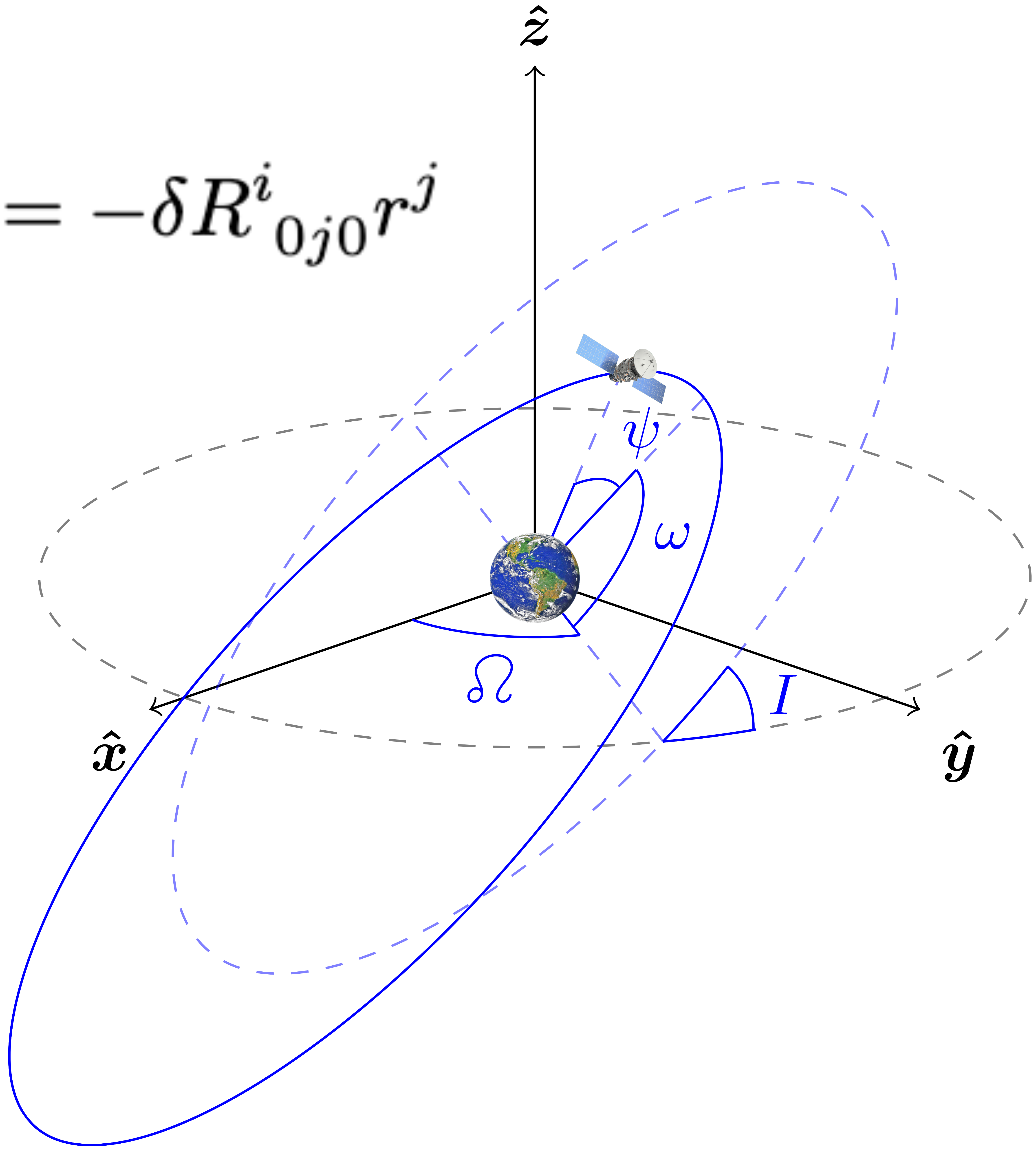

- **period** P**, eccentricity** e:
  size and *shape* of orbit
- **inlination** I**, ascending node** Ω:
  orientation in space
- **pericentre** ω**,**
  mean anomaly at epoch ε:
  radial and angular *phases*

Osculating orbits

$$\ddot{\boldsymbol{r}} + \frac{GM}{r^2}\hat{\boldsymbol{r}} = \delta\ddot{\boldsymbol{r}}.$$

- for generic acceleration:

$$\delta\ddot{\boldsymbol{r}} = r(\mathcal{F}_r\hat{\boldsymbol{r}} + \mathcal{F}_\theta\hat{\boldsymbol{\theta}} + \mathcal{F}_\ell\hat{\boldsymbol{\ell}}),$$

$$\dot{P} = \frac{3P^2\gamma}{2\pi}\left[\frac{e\sin\psi\mathcal{F}_r}{1+e\cos\psi} + \mathcal{F}_\theta\right],$$

$$\dot{e} = \frac{\dot{P}\gamma^2}{3Pe} - \frac{P\gamma^5\mathcal{F}_\theta}{2\pi e(1+e\cos\psi)^2},$$

$$\dot{I} = \frac{P\gamma^3\cos\theta\mathcal{F}_\ell}{2\pi(1+e\cos\psi)^2},$$

$$\dot{\Omega} = \frac{\tan\theta}{\sin I}\dot{I},$$

$$\dot{\omega} = \frac{P\gamma^3}{2\pi e}\left[\frac{(2+e\cos\psi)\sin\psi\mathcal{F}_\theta}{(1+e\cos\psi)^2} - \frac{\cos\psi\mathcal{F}_r}{1+e\cos\psi}\right] - \cos I\dot{\Omega},$$

$$\dot{\varepsilon} = -\frac{P\gamma^4\mathcal{F}_r}{\pi(1+e\cos\psi)^2} - \gamma(\cos I\dot{\Omega} + \dot{\omega}),$$

Osculating orbits

$$\ddot{\boldsymbol{r}} + \frac{GM}{r^2}\hat{\boldsymbol{r}} = \delta\ddot{\boldsymbol{r}}.$$

- for generic acceleration:

$$\delta\ddot{\boldsymbol{r}} = r(\mathcal{F}_r\hat{\boldsymbol{r}} + \mathcal{F}_\theta\hat{\boldsymbol{\theta}} + \mathcal{F}_\ell\hat{\boldsymbol{\ell}}),$$

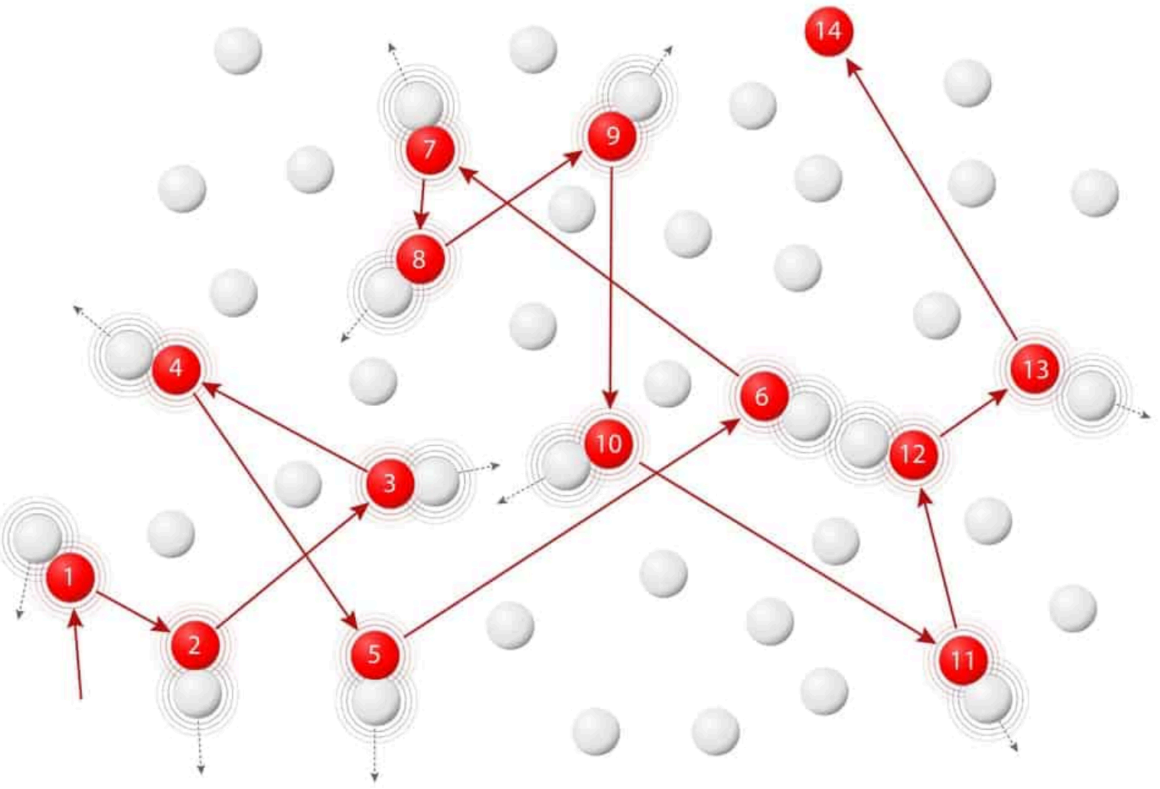

$$\dot{P} = \frac{3P^2\gamma}{2\pi}\left[\frac{e\sin\psi\mathcal{F}_r}{1+e\cos\psi} + \mathcal{F}_\theta\right],$$

$$\dot{e} = \frac{\dot{P}\gamma^2}{3Pe} - \frac{P\gamma^5\mathcal{F}_\theta}{2\pi e(1+e\cos\psi)^2},$$

$$\dot{I} = \frac{P\gamma^3\cos\theta\mathcal{F}_\ell}{2\pi(1+e\cos\psi)^2},$$

$$\dot{\Omega} = \frac{\tan\theta}{\sin I}\dot{I},$$

$$\dot{\omega} = \frac{P\gamma^3}{2\pi e}\left[\frac{(2+e\cos\psi)\sin\psi\mathcal{F}_\theta}{(1+e\cos\psi)^2} - \frac{\cos\psi\mathcal{F}_r}{1+e\cos\psi}\right] - \cos I\dot{\Omega},$$

$$\dot{\varepsilon} = -\frac{P\gamma^4\mathcal{F}_r}{\pi(1+e\cos\psi)^2} - \gamma(\cos I\dot{\Omega} + \dot{\omega}),$$

But the effect is stochastic… Fokker-Planck approach

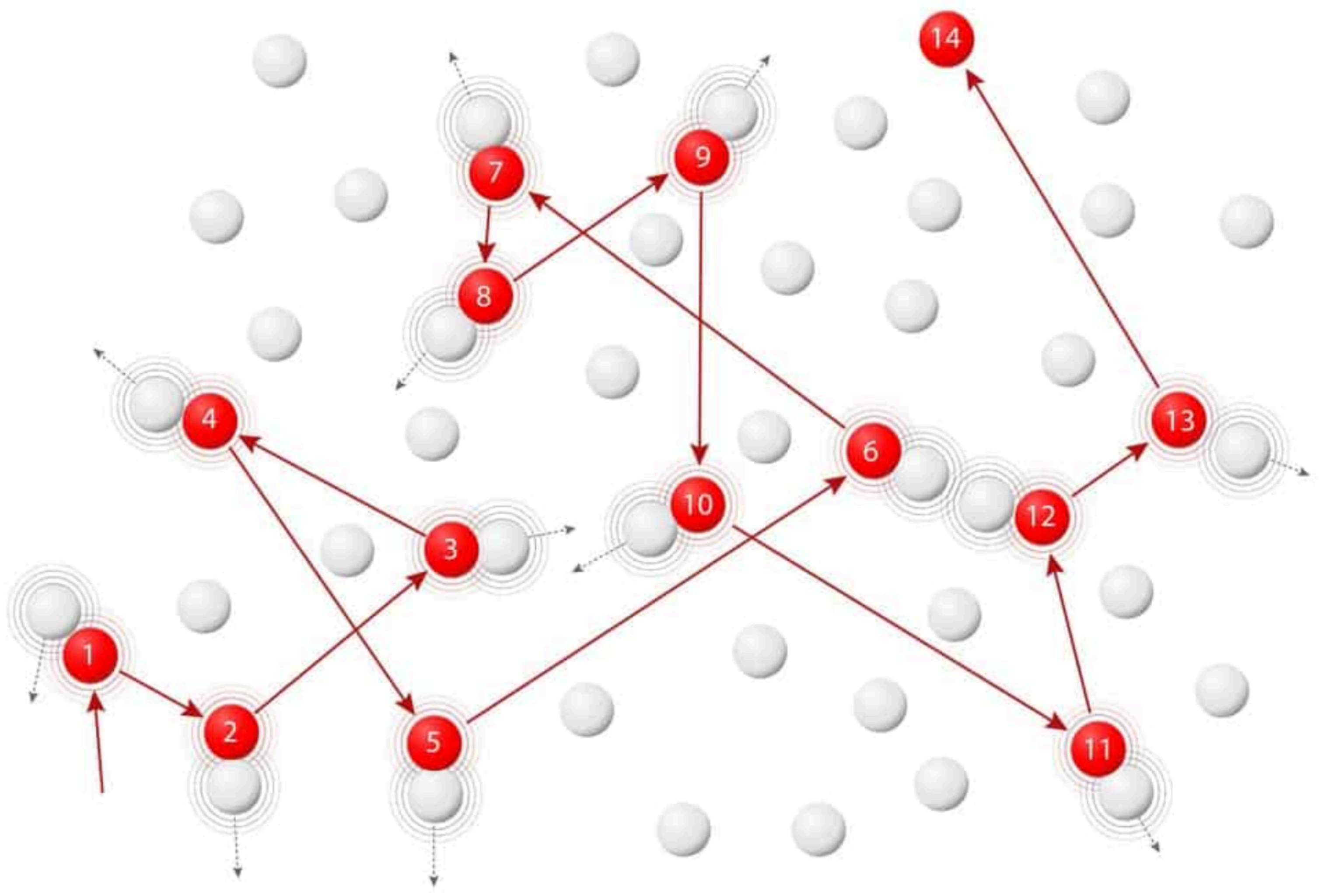

deterministic

stochastic

$$\dot{X}_i(\boldsymbol{X},t) = V_i(\boldsymbol{X}) + \Gamma_i(\boldsymbol{X},t),$$

we move from dynamics of the variable to dynamics of the **distribution *W(X)***

Fokker-Planck averaged over orbits

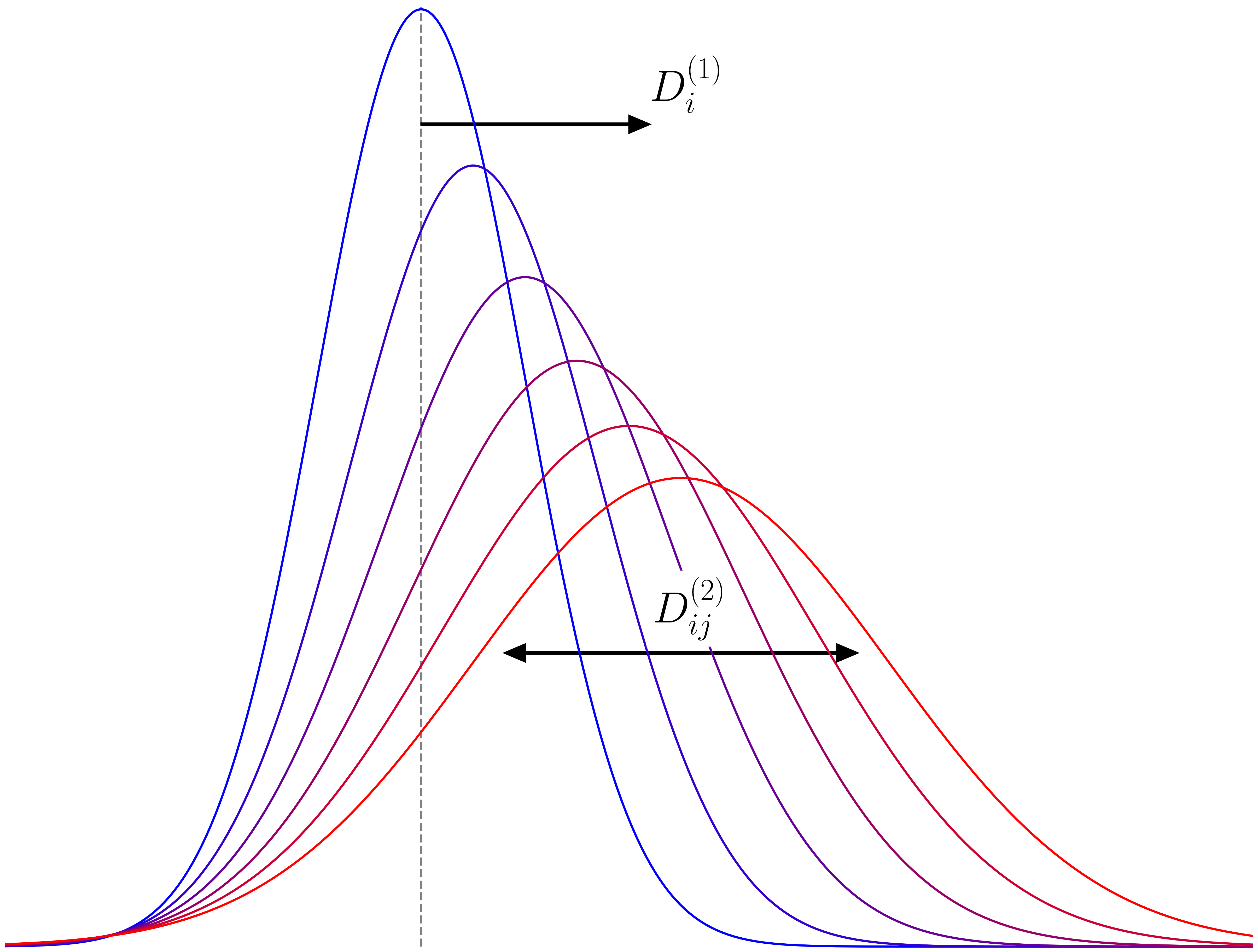

- track distribution function $W(\boldsymbol{X}, t)$ of orbital elements $\boldsymbol{X} = (P, e, I, \Omega, \omega, \varepsilon)$
- evolves through *Fokker-Planck eqn.*

$$\frac{\partial W}{\partial t} = -\frac{\partial}{\partial X_i}\left(D_i^{(1)} W\right) + \frac{\partial}{\partial X_i}\frac{\partial}{\partial X_j}\left(D_{ij}^{(2)} W\right)$$

- *drift* and *diffusion* coefficients (averaged over orbits)

$$D_i^{(1)}(\boldsymbol{X}) = V_i(\boldsymbol{X}) + \sum_{n=1}^{\infty} \mathcal{A}_{n,i}(\boldsymbol{X})\Omega_{\rm gw}(n/P)$$

$$D_{ij}^{(2)}(\boldsymbol{X}) = \sum_{n=1}^{\infty} \mathcal{B}_{n,ij}(\boldsymbol{X})\Omega_{\rm gw}(n/P)$$

Two binary probes

timing of binary pulsars

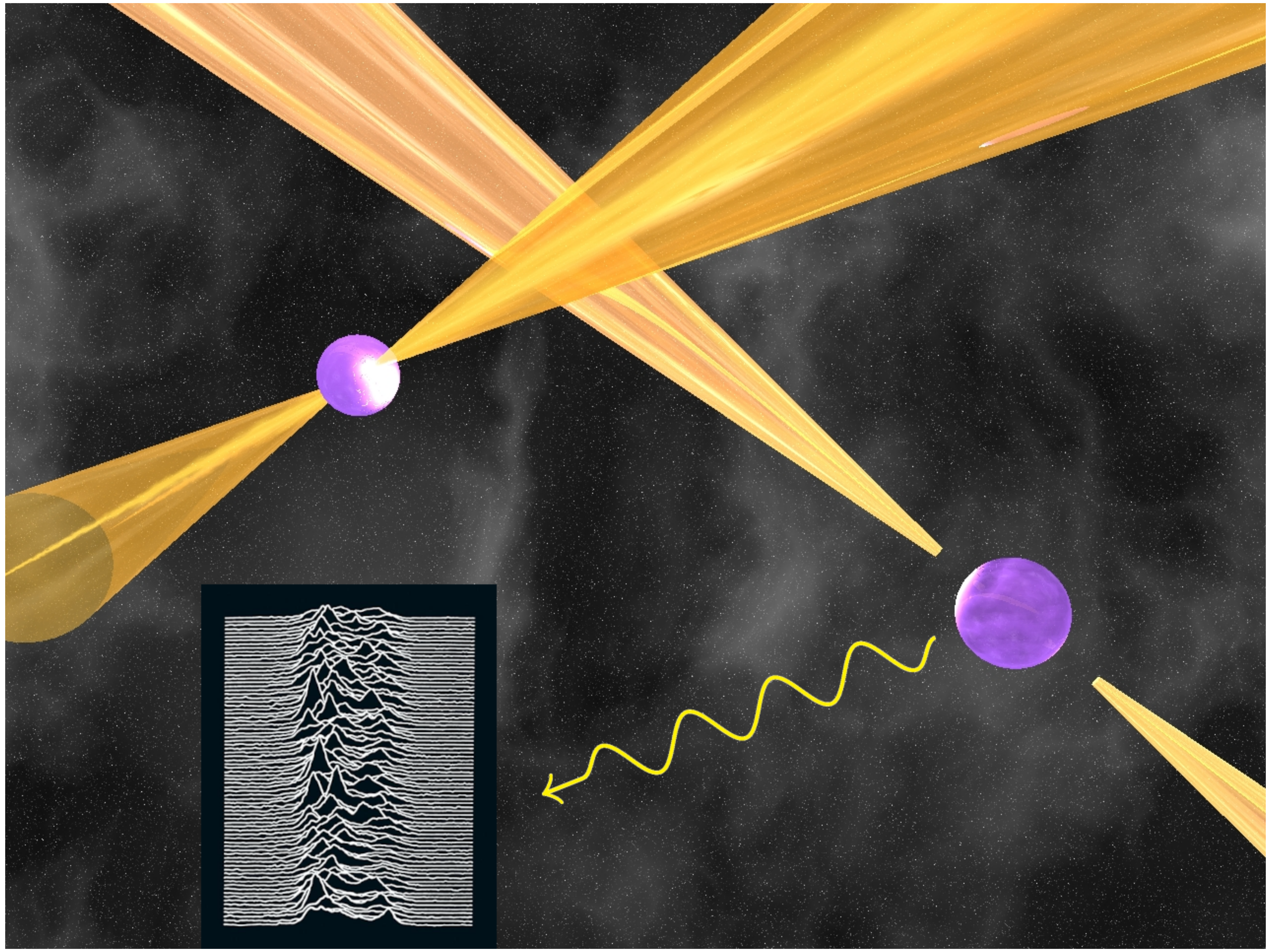

(pulsar animation credit: Michael Kramer)

lunar and satellite laser ranging

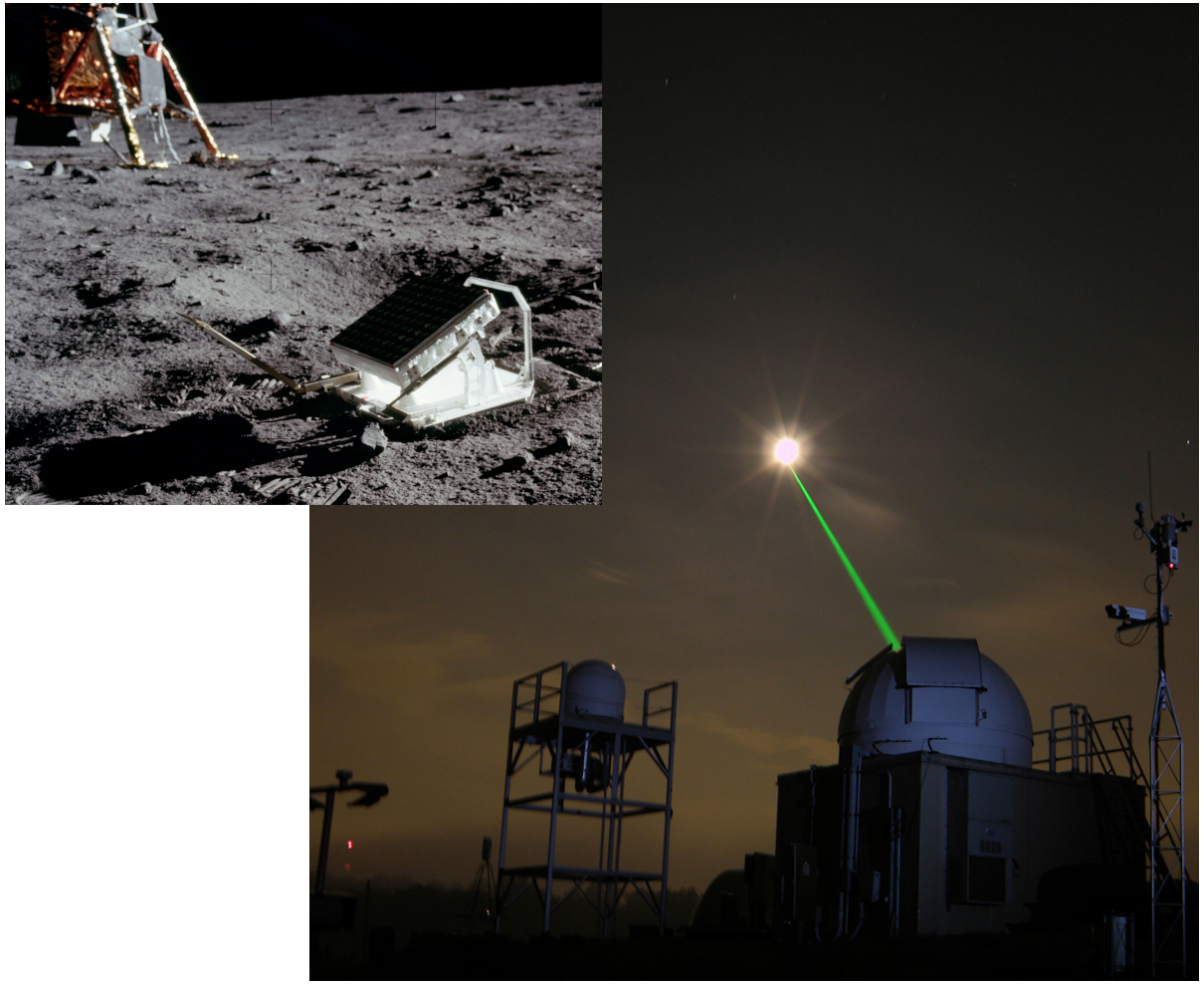

(image credit: NASA)

Our forecast constraints

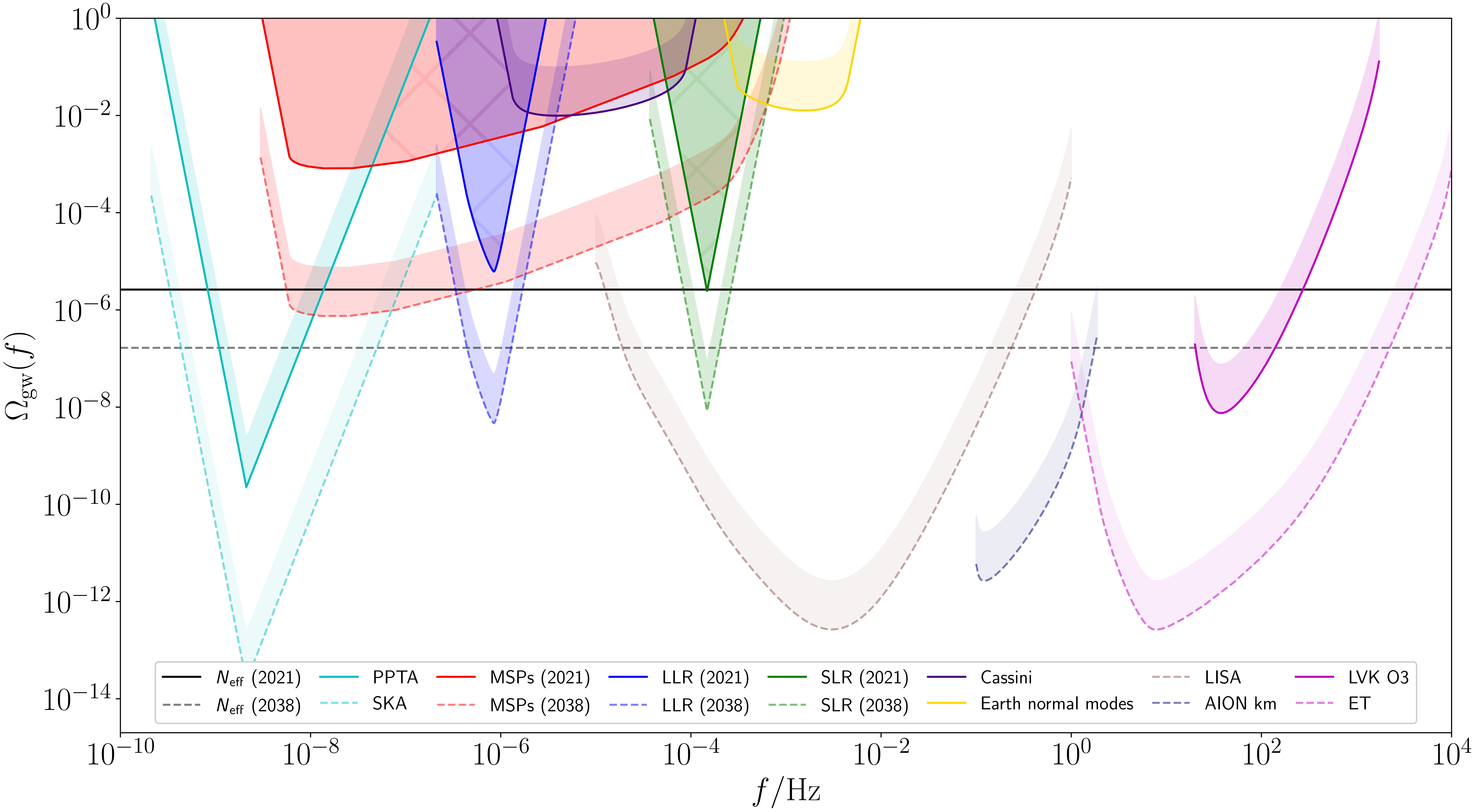

Signals in the μHz band

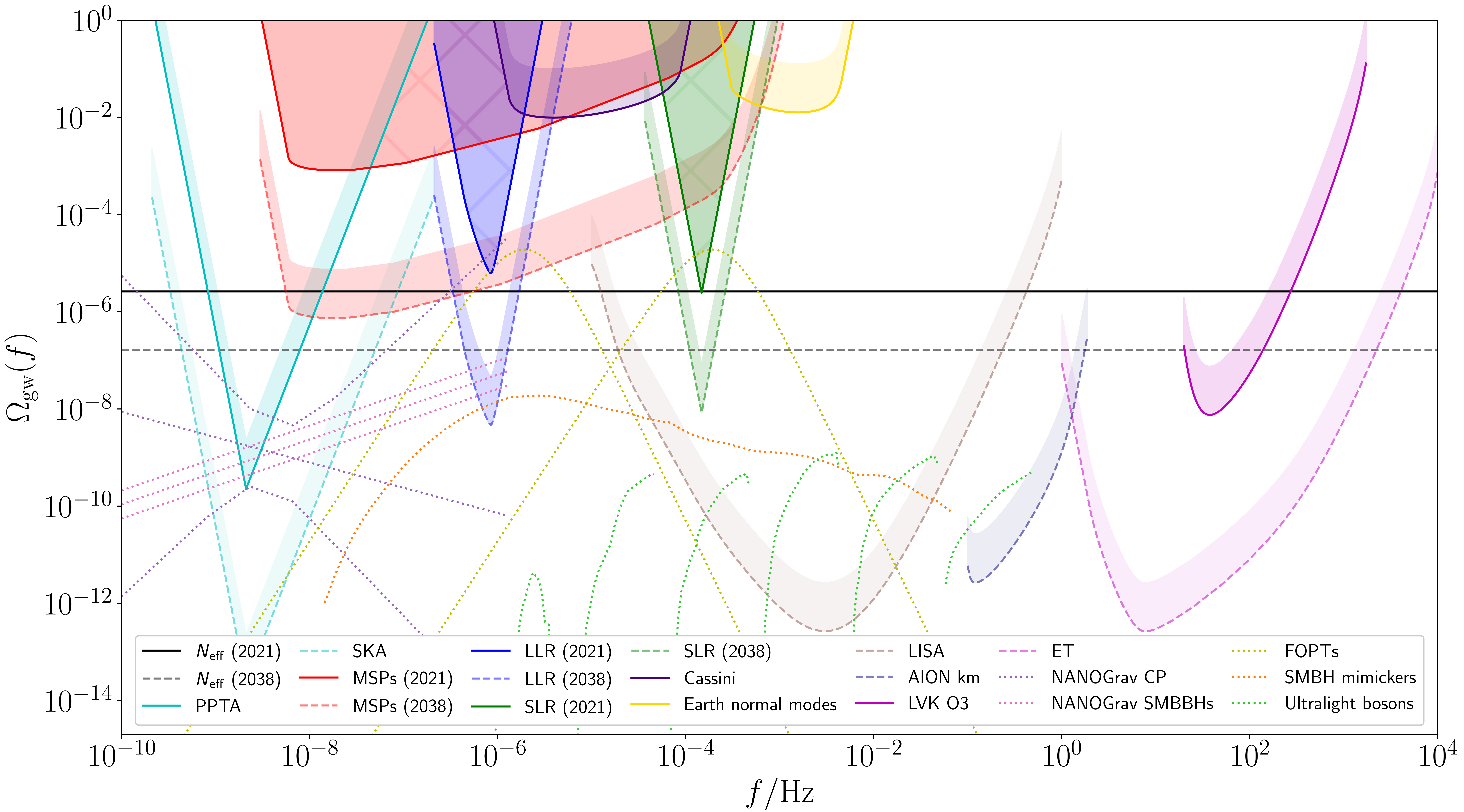

dblas@ifae.es

Summary and outlook (part I)

- binary resonance can probe a unique GW frequency band
- we have developed a powerful new formalism
- unique constraints on phase transitions (and more)
- plenty more work to do! more signals, more systems, plus running on real data

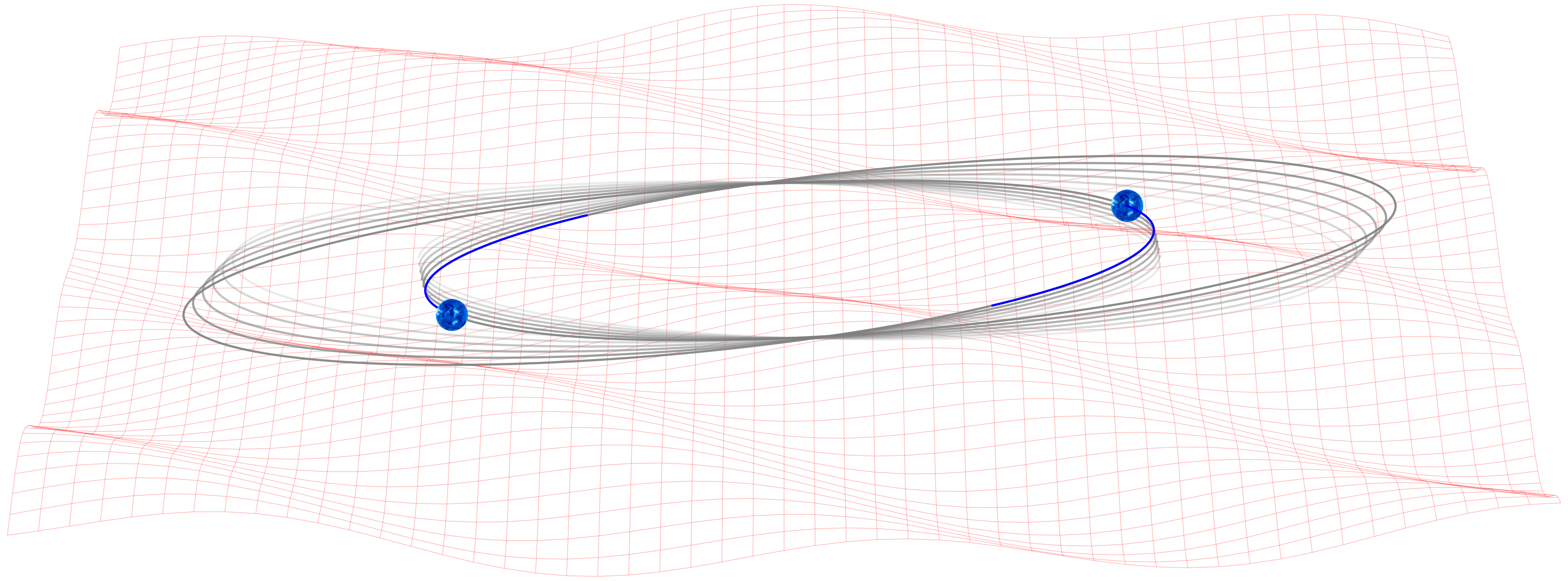

part I: μHz

part II: GHz

The Gravitational Soundscape

Kite 22

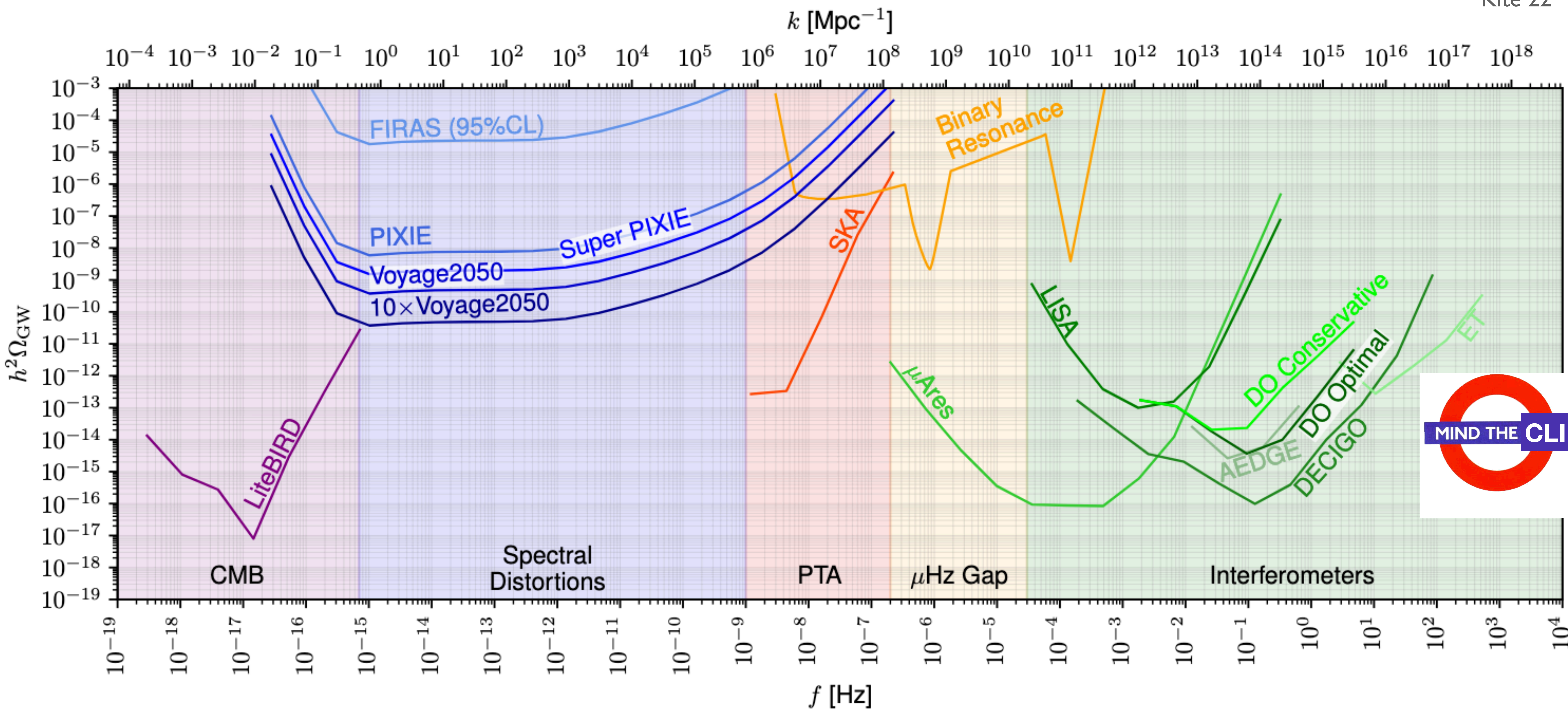

MIND THE CLIFF

The Gravitational Soundscape *at high frequencies*

Crucial question: what sources above kHz?

review
Aggarwal et al, 2011.12414

	Stochastic	Coherent
Standard Model:	✓ Thermal plasma fluctuations Ghiglieri & Laine (2015) Ghiglieri et al (2020) Ringwald et al (2020)	✗ ?
BSM:	✓ Inflation Phase transitions Cosmic Strings …	✓ PBH inspirals Superradiance Exotic objects …

The Gravitational Soundscape *at high frequencies*

SMASH model full spectrum

Ringwald Tamarit 22

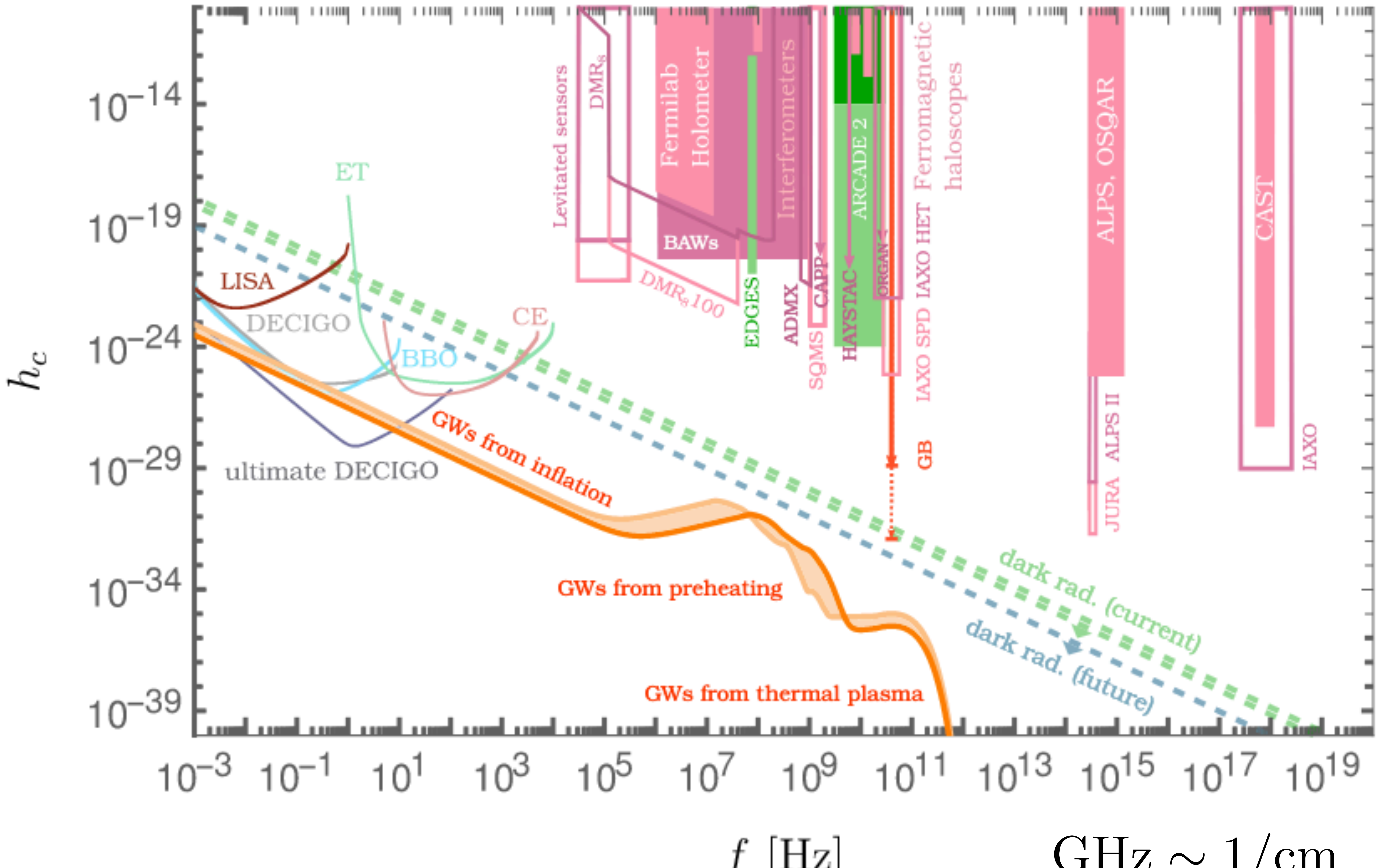

$\mathrm{GHz} \sim 1/\mathrm{cm}$

$\delta L \sim hL$

Searching for GWs with light

Interaction GWs with light

$$\mathcal{L} = \sqrt{-g}\,(R + F_{\mu\nu}F^{\mu\nu}) \supset \frac{1}{2}A_\mu j^\mu_{\rm eff}(h) + \eta^{\mu\alpha}\eta^{\nu\beta}F_{\mu\nu}F_{\alpha\beta} + O(h^2)$$

$$j^\mu_{\rm eff} = -\partial_\beta\left(\frac{1}{2}hF^{\mu\beta} + h^\beta_\alpha F^{\alpha\mu} - h^\mu_\alpha F^{\alpha\beta}\right)$$

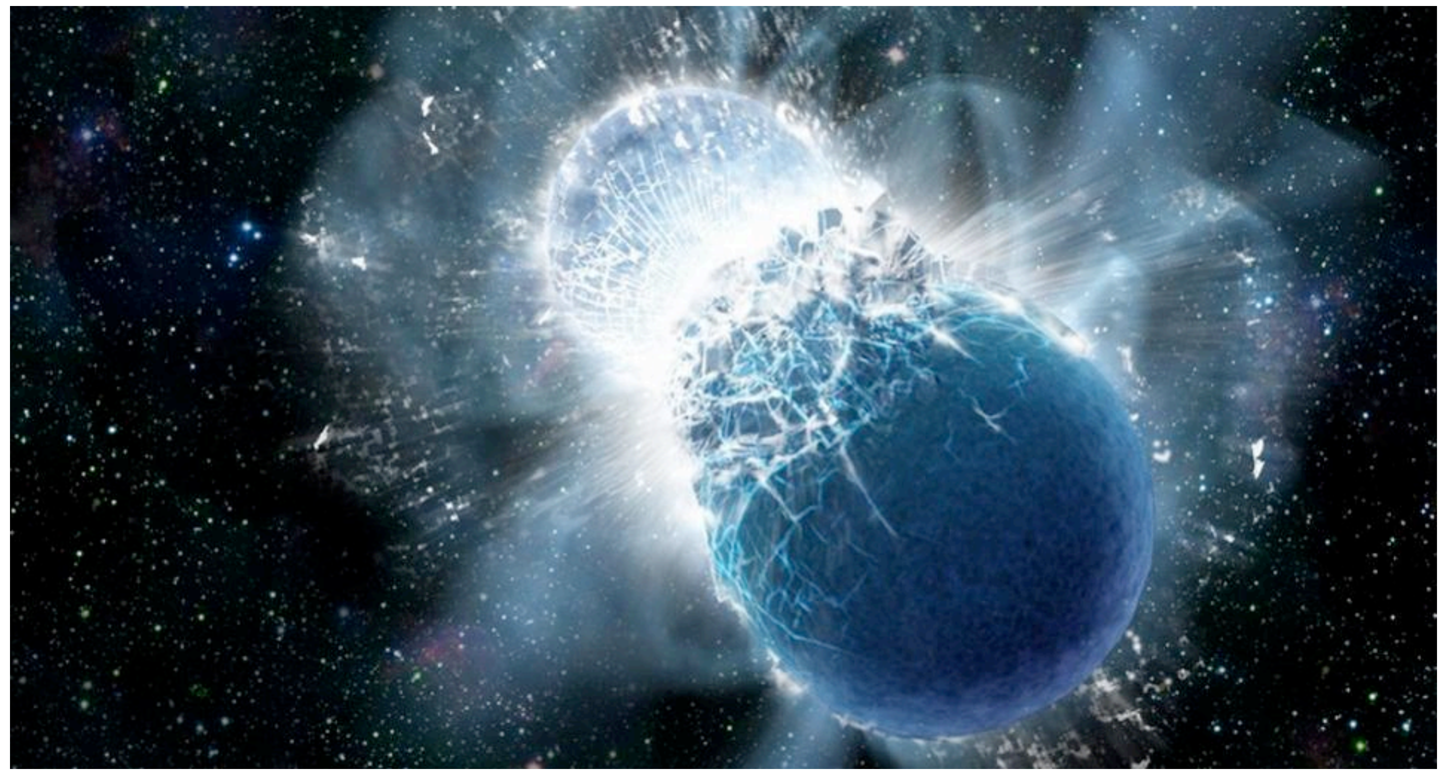

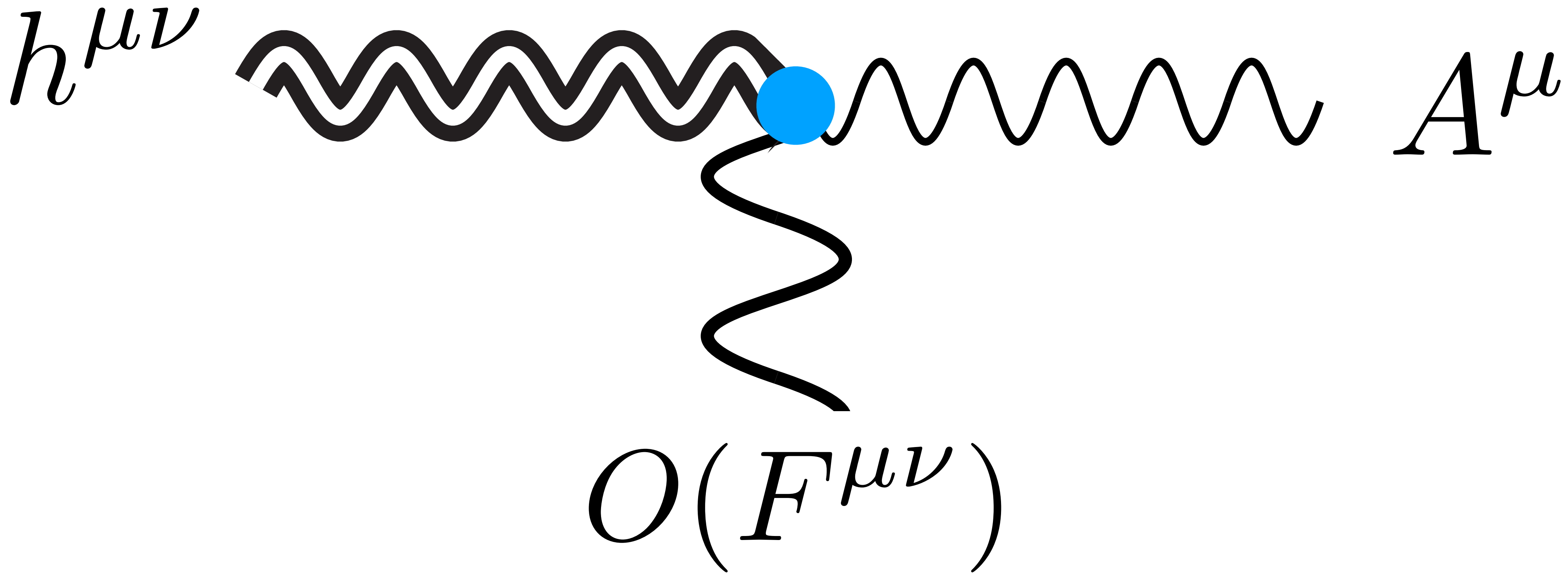

What are we looking for?

Interaction GWs with light

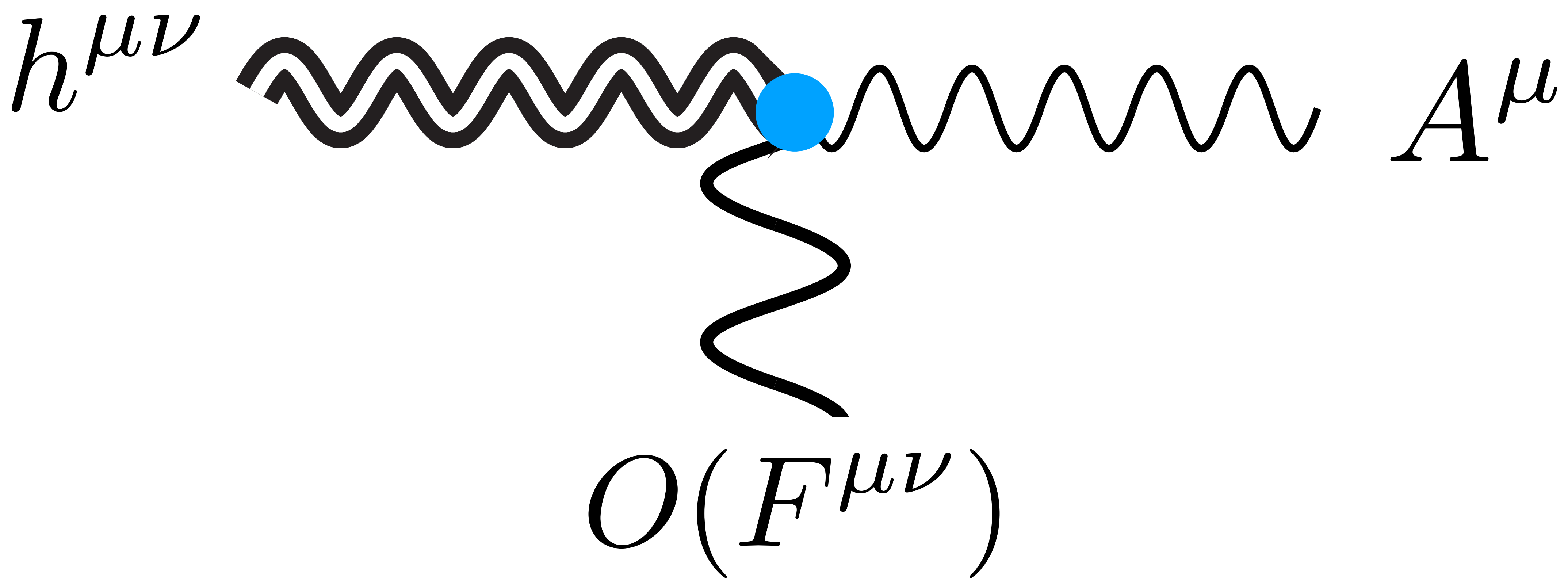

analogy with axions

$$a\tilde{F}F$$

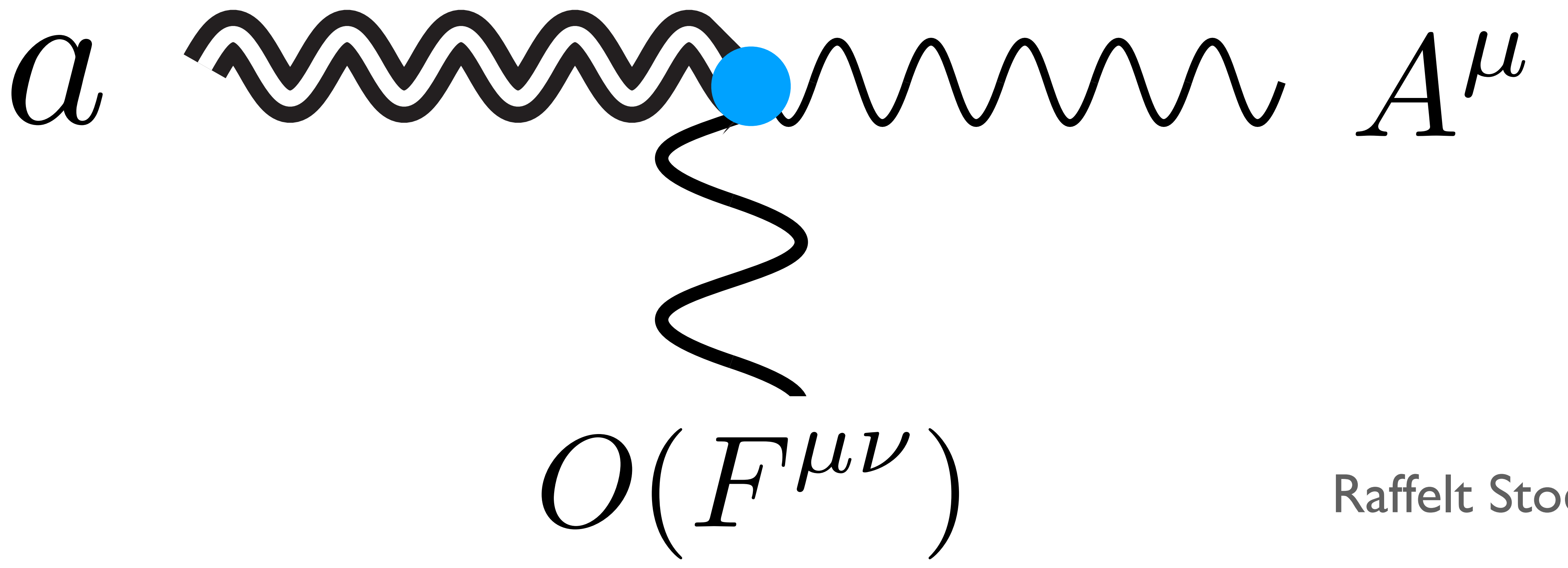

Raffelt Stodolsky 87

How does this happen?

Cavities

MAGO design from CERN (gr-qc/0502054)
we are revisiting it…

EM-coupling

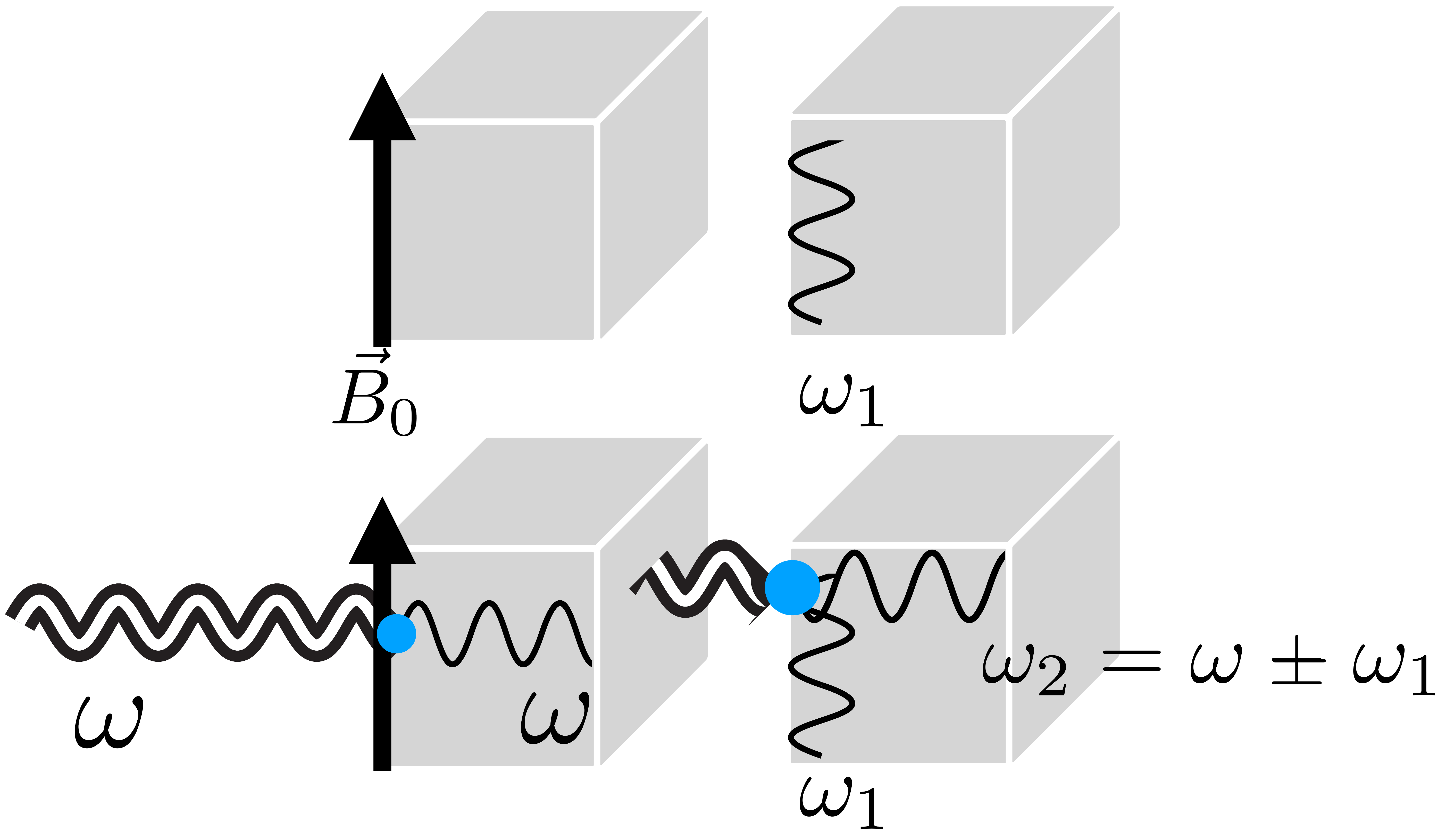

Mechanical-coupling
(shaking the walls)

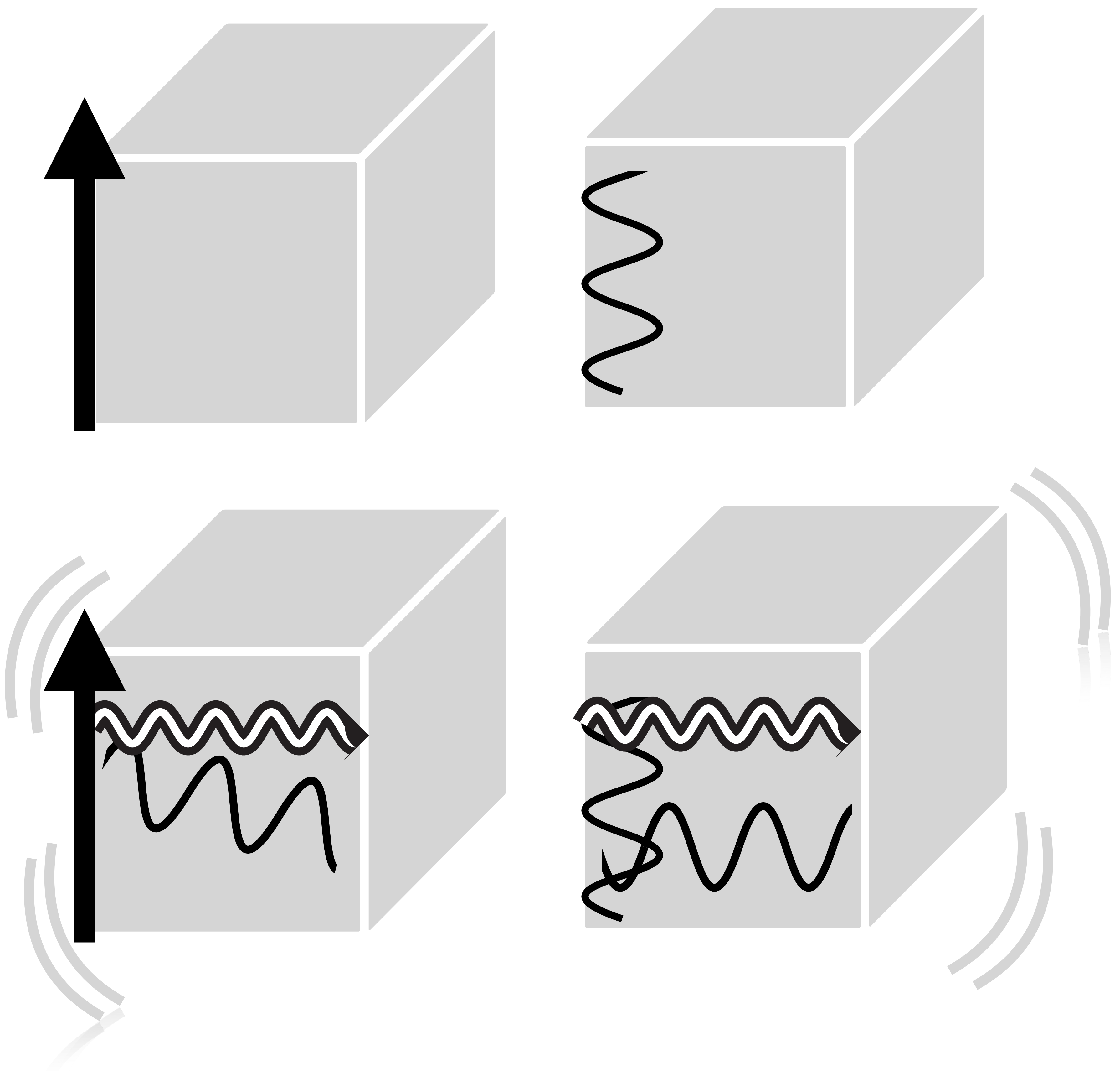

How does this happen?

Cavities

MAGO design f om CERN (gr-qc/0502054)
we are revisiting it…

EM-coupling

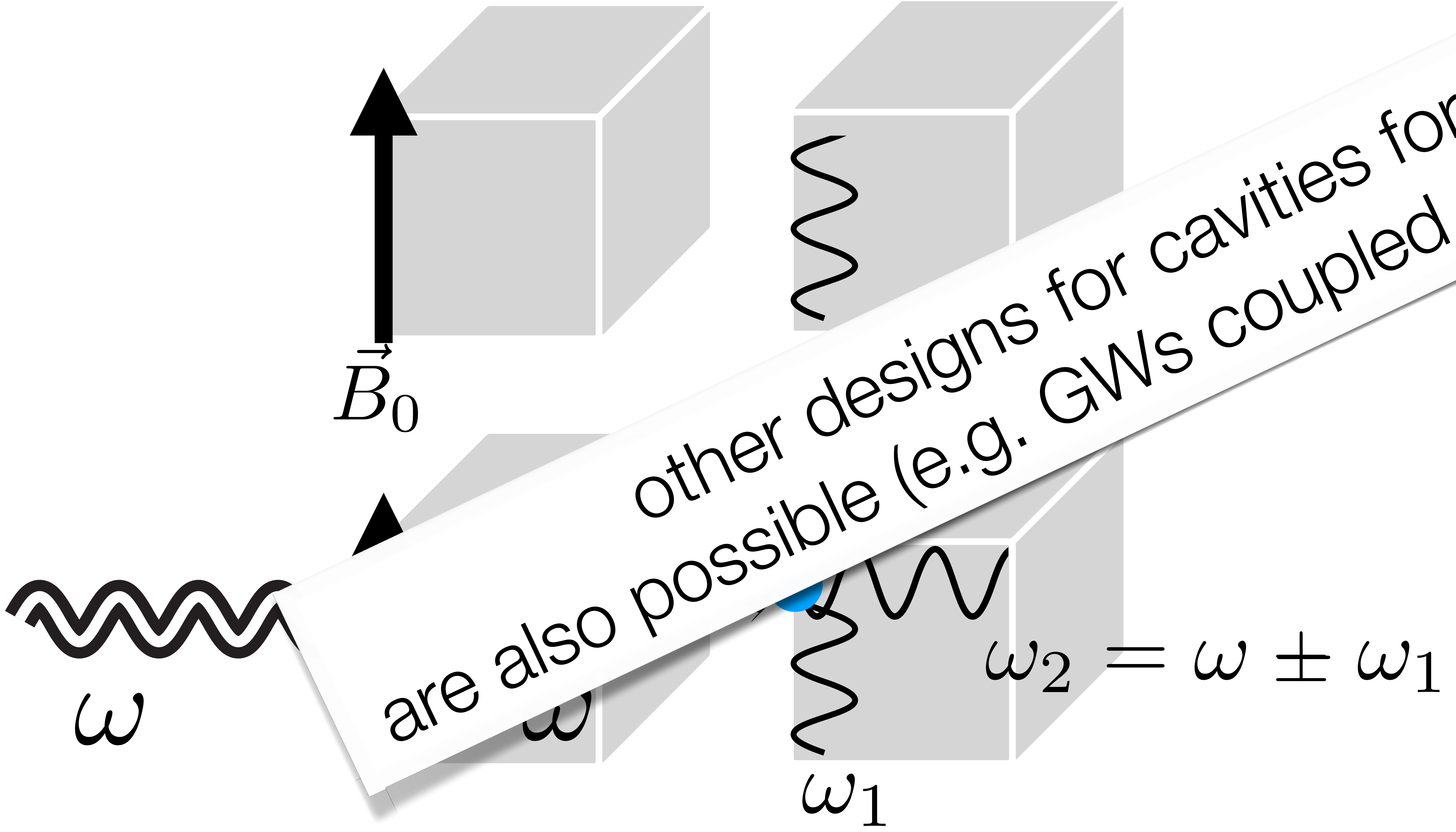

Mech pling
walls)

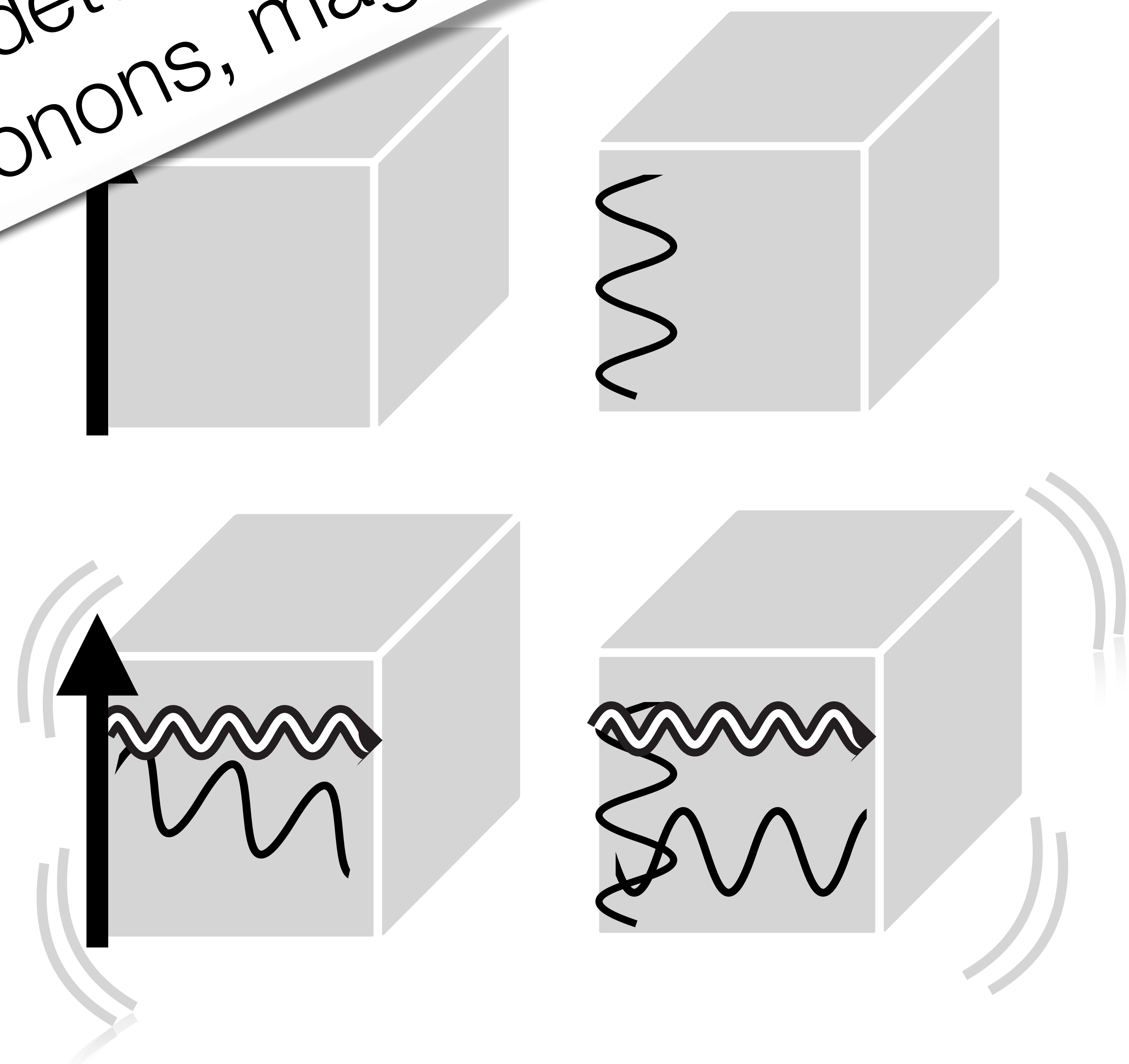

other designs for cavities for GW detection
are also possible (e.g. GWs coupled to phonons, magnons,…)

Some details

$$g_{\mu\nu} = \eta_{\mu\nu} + h^{LIF}_{\mu\nu}$$

i) choice of frame

Marzlin, 94

Local inertial frame (LIF) geodesic $\rightarrow$ Laboratory frame

$$\ddot{z}^\mu + \Gamma^\mu_{\nu\lambda}\dot{z}^\nu\dot{z}^\lambda = a^\mu$$

laboratory coordinates accelerated wrt LIF

Some details

$$g_{\mu\nu} = \eta_{\mu\nu} + h^{LIF}_{\mu\nu}$$

i) choice of frame

Marzlin, 94

Local inertial frame (LIF)
geodesic

Laboratory frame

$$\ddot{z}^\mu + \Gamma^\mu_{\nu\lambda}\dot{z}^\nu\dot{z}^\lambda = a^\mu$$

laboratory coordinates accelerated wrt LIF

Some details

$R \sim \omega^2 h$

i) choice of frame $R_{\mu\nu\rho\sigma}(h) = R_{\mu\nu\rho\sigma}(h^{TT}) + O(h^2)$

LIF at order $O((\omega L)^3)$

$$h_{00}^{\text{LIF}} \simeq -R_{0i0j}x^i x^j \quad , \quad h_{ij}^{\text{LIF}} \simeq -\frac{1}{3}R_{ikjl}x^k x^l, \quad h_{0i}^{\text{LIF}} \simeq -\frac{2}{3}R_{0jik}x^j x^k$$

Some details

$$R \sim \omega^2 h$$

i) choice of frame $R_{\mu\nu\rho\sigma}(h) = R_{\mu\nu\rho\sigma}(h^{TT}) + O(h^2)$

LIF at order $O((\omega L)^3)$

$$h_{00}^{\text{LIF}} \simeq -R_{0i0j}x^i x^j \quad , \quad h_{ij}^{\text{LIF}} \simeq -\frac{1}{3}R_{ikjl}x^k x^l, \quad h_{0i}^{\text{LIF}} \simeq -\frac{2}{3}R_{0jik}x^j x^k$$

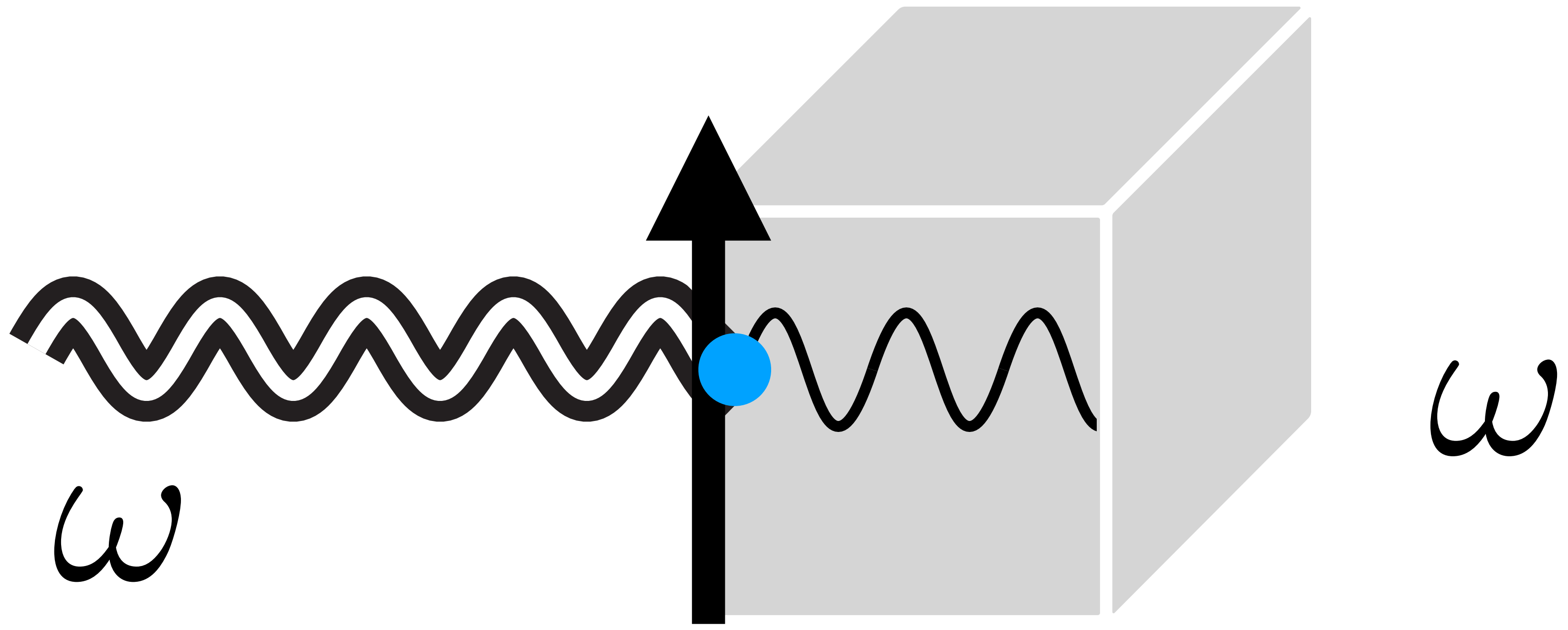

Some details

$R \sim \omega^2 h$

i) choice of frame $\quad R_{\mu\nu\rho\sigma}(h) = R_{\mu\nu\rho\sigma}(h^{TT}) + O(h^2)$

LIF at order $\quad O((\omega L)^3)$

$$h_{00}^{\text{LIF}} \simeq -\cancel{R_{0i0j}x^i x^j} \quad , \quad h_{ij}^{\text{LIF}} \simeq -\frac{1}{3}\cancel{R_{ikjl}x^k x^l}, \quad h_{0i}^{\text{LIF}} \simeq -\frac{2}{3}\cancel{R_{0jik}x^j x^k}$$

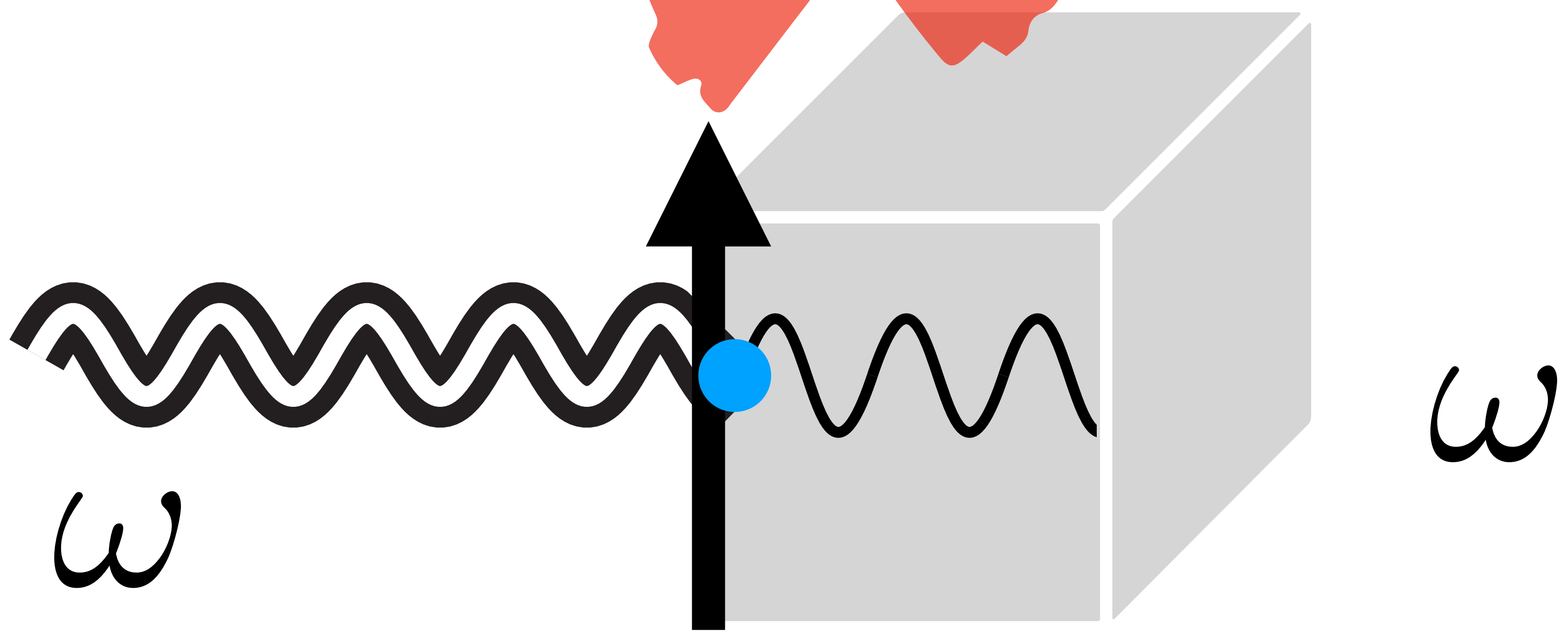

$$\omega_r \sim \lambda^{-1} \sim L^{-1}$$

Some (VERY IMPORTANT) details

LIF at all order in $h^{\mu\nu}$

Marzlin, 94

and it can be resummed for a GW!!

A. Berlin, DB, R.T. D'Agnolo, S. Ellis, R. Harnik, Y. Kahn, J. Schütte-Engel

$$h_{00} = -R_{0i0j}\, x^i\, x^j \times 2\left[-\frac{i}{\omega_g z} + \frac{1-e^{-i\omega_g z}}{(\omega_g z)^2}\right]$$

$$h_{ij} = -\frac{1}{3} R_{ikjl}\, x^k\, x^l \times 6\left[-\frac{1+e^{-i\omega_g z}}{(\omega_g z)^2} - 2i\,\frac{1-e^{-i\omega_g z}}{(\omega_g z)^3}\right]$$

$$h_{0i} = -\frac{2}{3} R_{0jik}\, x^j\, x^k \times 3\left[-\frac{i}{2\,\omega_g z} - \frac{e^{-i\omega_g z}}{(\omega_g z)^2} - i\,\frac{1-e^{-i\omega_g z}}{(\omega_g z)^3}\right]$$

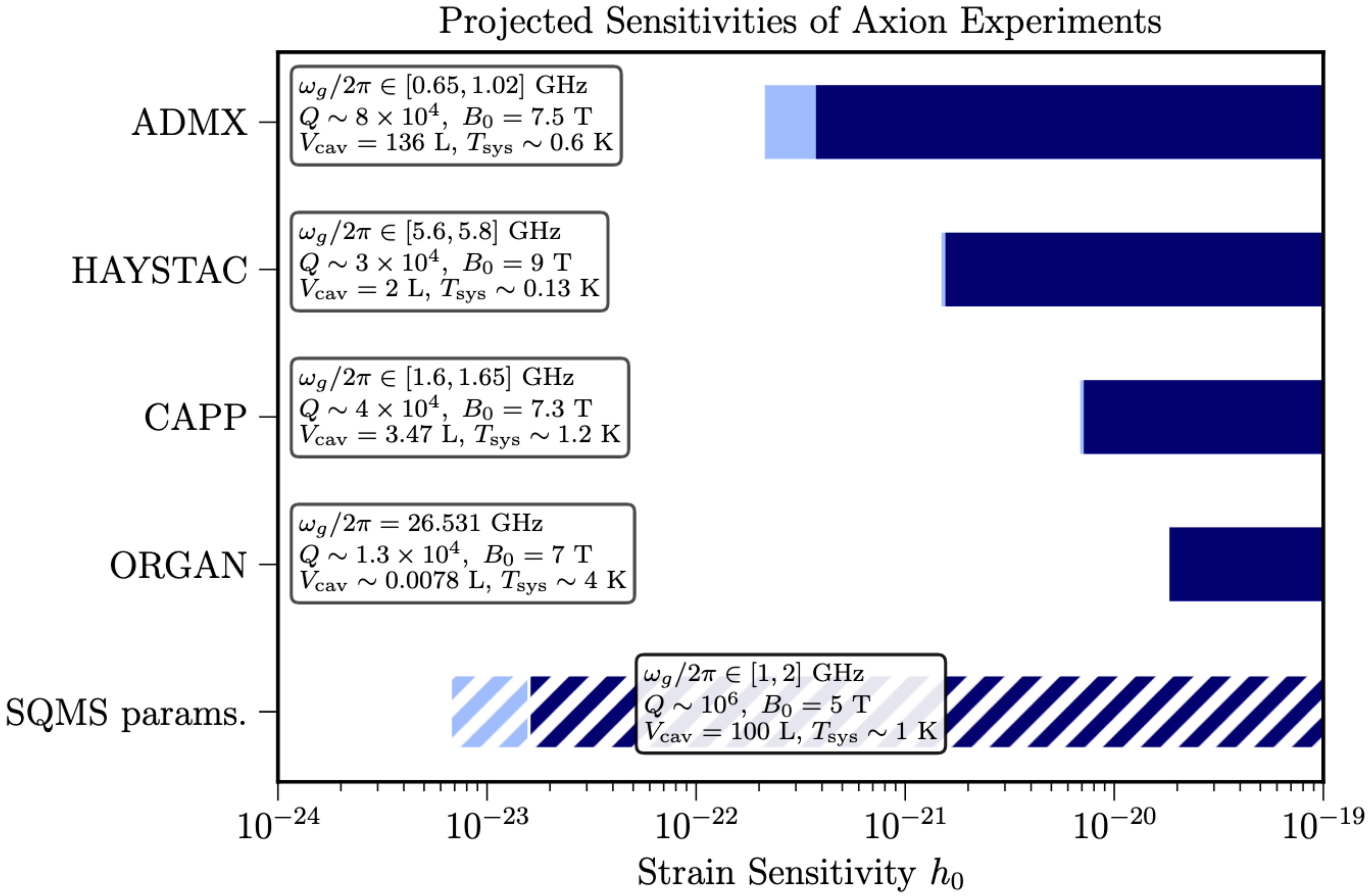

+ it's directional and not degenerate with axions

The Gravitational Soundscape *at high frequencies*

GWs from PBHs (rates 1/year)

SMASH model full spectrum

Ringwald Tamarit 22

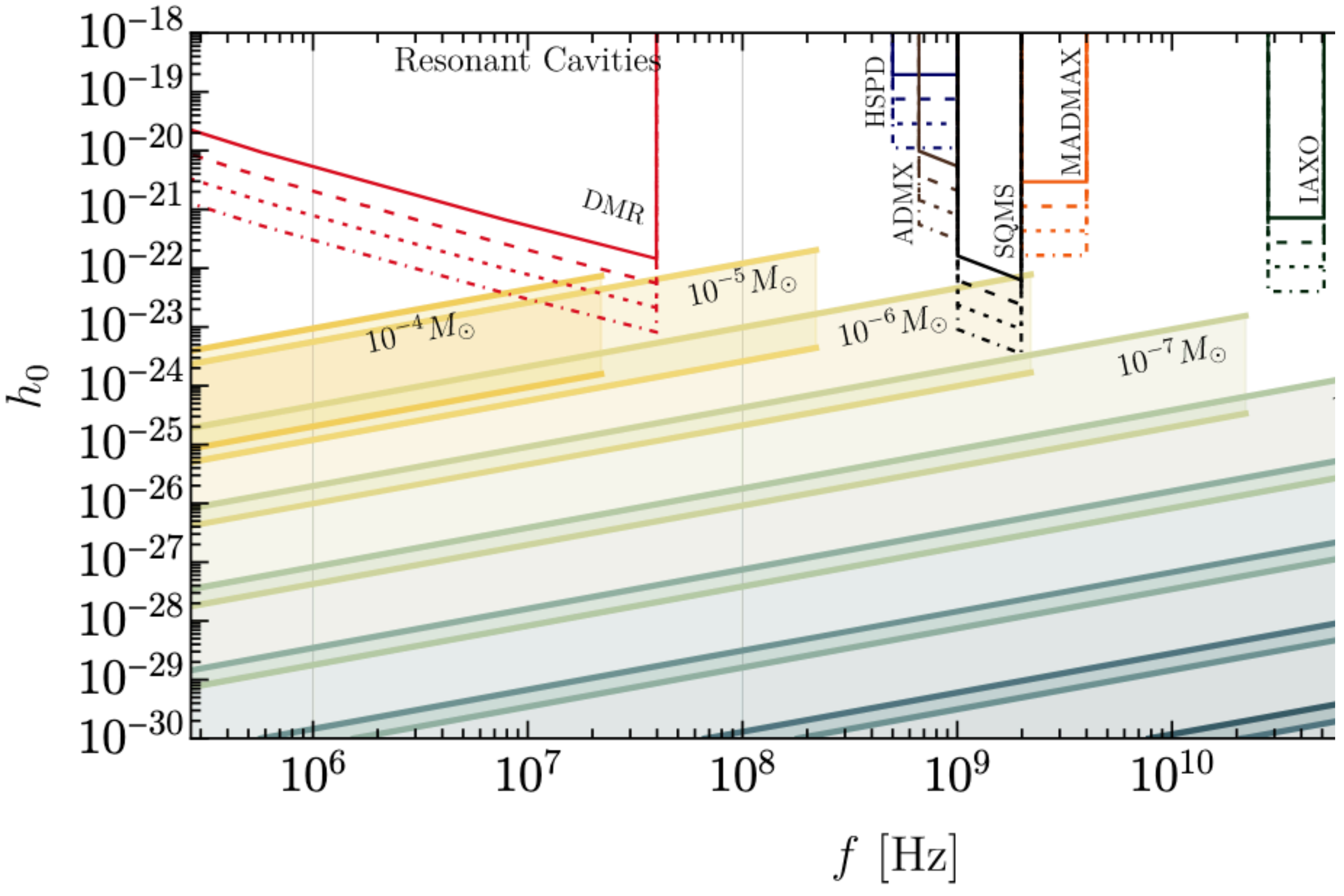

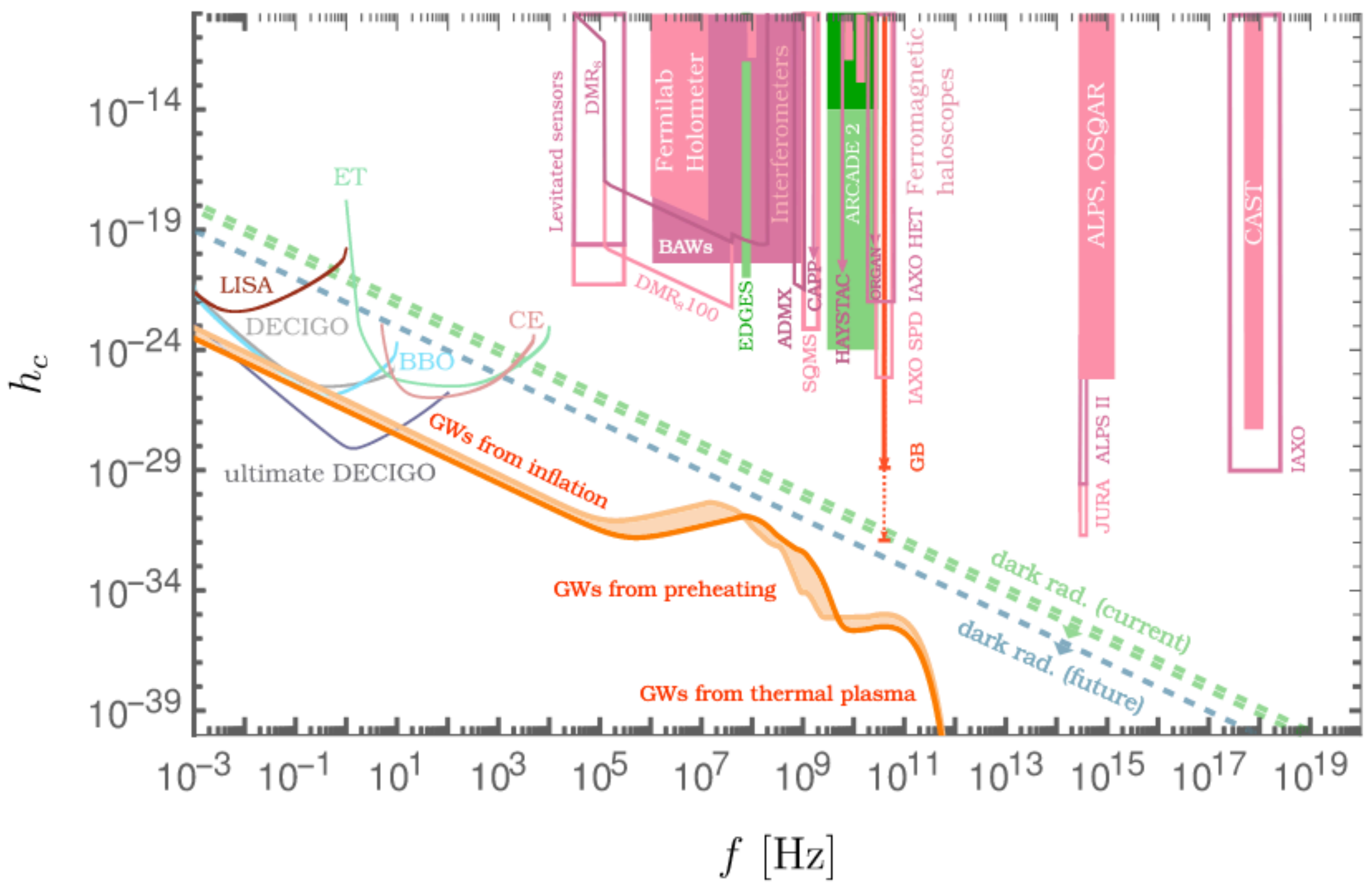

Conclusions (part II)

- SRF cavities are a mature technology to look for GWs at GHz either
    - 'ADMX' like
    - Heterodyne

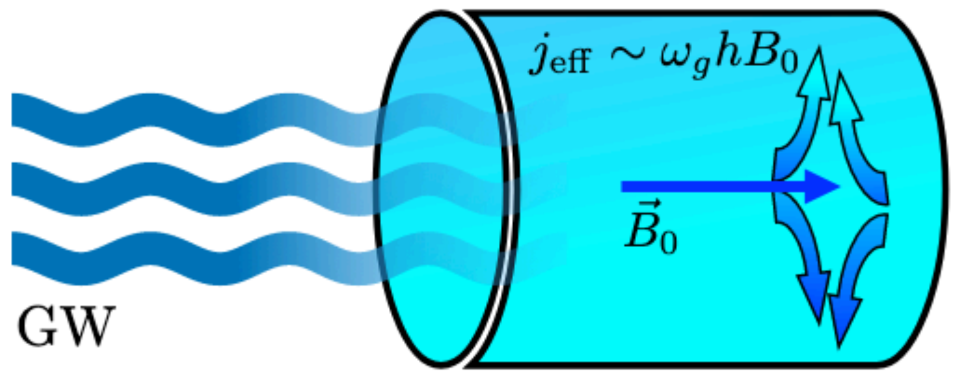

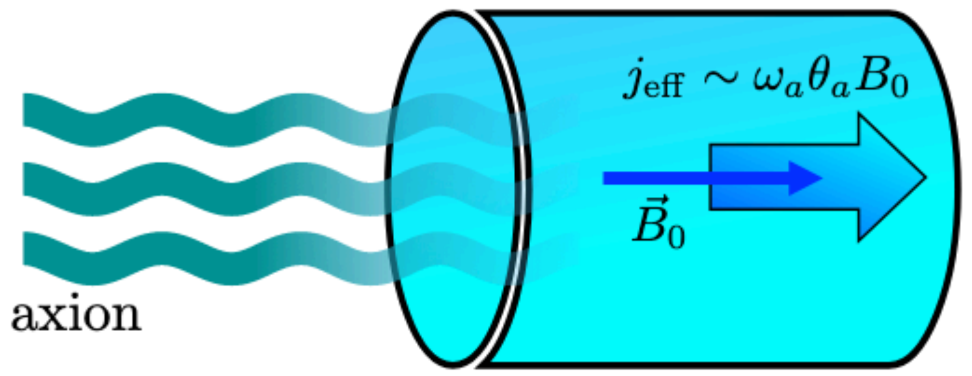

- As in any GR calculation: subtleties in working with a consistent gauge
    - TT gauge needs to be converted to laboratory frame
    - The laboratory frame may need all orders in $\sim O((\omega L))$

- In the laboratory frame, there is sensitivity to ALL directions! (also longitudinal)
- Stay tuned for the connection to real world… (noise estimates + prospects)